Does shift in trophic strategy contribute to an enhanced bleaching resilience of corals regularly exposed to upwelling?

M.Sc. Thesis in Biological Oceanography

by

Merlin Weichler

Matrikel-Nr. 1037078

29th of February, 2024

Supervision by

Prof. Dr. Frank Melzner

Dr. Marlene Wall

Deutsche Zusammenfassung

In der Andamanensee treten regelmäßig interne Wellen von außergewöhnlicher Größe und Häufigkeit auf. Diese brechen am Kontinentalschelf und befördern regelmäßig kaltes, nährstoffreiches, hypoxisches Tiefseewasser in die Oberflächenschicht. Die Inseln der Andamanensee schützen die Korallenriffe vor den Auswirkungen dieser internen Wellen mit großer Amplitude (Large amplitude internal waves = LAIW) an der Ostküste und trennen sie von den exponierten Riffen an der Westküste. Die exponierten Riffe beherbergen Korallen mit erhöhter Bleicheresistenz, aber es ist noch nicht klar, welche Prozesse diese Resistenzen ermöglichen. Da sich gezeigt hat, dass heterotrophe Ernährung eine wichtige Rolle bei der Widerstandsfähigkeit von Warmwasserkorallen spielt, könnte eine Verschiebung der trophischen Strategie Aufgrund des angereicherten Fluss an organischem Material durch LAIW zur Wärmeresistenz beitragen. In dieser Masterarbeit habe ich moderne stabile Isotopen- und Fettsäureanalytik an getrennten Korallenwirts- und Symbiodiniumfraktionen angewendet. Ziel war es die trophische Strategie der beiden Korallenarten *Porites lutea* und *Pocillopora verrucosa* von exponierten und geschützten Riffen der zwei Inseln Miang und Racha zu analysieren. Die Ergebnisse zeigen ein sehr komplexes Schema mit Insel- sowie Artspezifischen Effekten. *Pocillopora* zeigt nur kleine Unterschiede in Fettsäure-Ernährungs- und Gesundheitsmarkern. Ernährungsmarker weisen auf eine geringfügig höhere Heterotrophie auf Rachas LAIW-exponiertem, aber auch auf Miangs geschütztem Standort hin. SIBER-Analyse an *Pocillopora* zeigt keine Unterschiede in der Ernährungsstrategie. *Porites* Fettsäuremarker zeigen dagegen eine Tendenz zu erhöhter Heterotrophie an Miangs LAIW exponiertem Standort und eine geringere Zunahme an Rachas exponierten Riffen. SIBER-Analyse beider Inseln zusammengenommen bestätigt dies jedoch nicht und weist stattdessen auf eine höhere Autotrophie von exponierten Korallen hin. Gesundheitsmarker in LAIW ausgesetzten *Porites* sind leicht erhöht. Zusammen mit erhöhter Biomasse und Fettsäuren pro Oberfläche weist dies auf einen gesünderen Phänotyp hin. LAIW exponierte *Pocillopora* hingegen zeigen diesen verbesserten Gesundheitsstatus nicht. Da das Verhalten zu mehr Heterotrophie nuanciert und kontextabhängig zu sein scheint, ist ein Wechsel der Ernährungsstrategie höchstwahrscheinlich nicht der treibende Faktor für die erhöhte Wärmeresistenz von LAIW-exponierten Korallen.

Abstract

In the Andaman Sea internal waves of extraordinary amplitudes and frequencies break at the continental shelf and periodically introduce cold, nutrient-rich, hypoxic deep-sea water into the surface layer. The islands of the Andaman Sea shelter coral reefs from the effects of these large amplitude internal waves (LAIW) on eastern shores and separate them from the exposed reefs on western shores. Exposed reefs harbor corals with increased heat resistance, but which processes facilitate this resistance is not yet clear. As heterotrophic feeding has been shown to play an important role in warm water coral bleaching resilience and recovery, a shift in trophic strategy through LAIW-enriched organic matter flux may contribute to thermal resistance. In this thesis I utilized modern stable isotope and fatty acid analytics on separated coral host and Symbiodinium fractions to assess the trophic strategy of two coral species *Porites lutea* and *Pocillopora verrucosa* from both shore sites of two islands in the Andaman Sea (Miang and Racha). The results reveal a complex picture, with island and species-specific effects. *Pocillopora* does not show large differences in fatty acid trophic and health markers, with trophic markers indicating marginal higher heterotrophy on Rachas LAIW exposed but also on Miangs sheltered site. SIBER analysis on *Pocillopora* signals consistent trophic strategy on both sides. *Porites* do show a tendency of increased heterotrophy on Miangs LAIW exposed site and a smaller increase on Rachas exposed reefs. However, SIBER analysis of both islands pooled does not support this and instead indicates higher autotrophy. Health markers in LAIW exposed *Porites* are slightly elevated, in concert with higher biomass and fatty acids per surface they suggest a healthier phenotype. However, *Pocillopora* does not demonstrate this enhanced health status with LAIW exposure. As shift towards more heterotrophy seems to be nuanced and context-dependent it is most likely not the driving factor for the elevated heating resistance observed in LAIW exposed corals.

Contents

List of Figures

List of Tables

Background

Coral reefs in a heating ocean

Coral reefs are among the most ecologically and economically valuable ecosystems. Although coral reefs only cover ~0.1% of the ocean floor they harbor more than a quarter of the ocean's biodiversity (Fisher et al., 2015). Coral reefs also provide a variety of ecosystem services to humans living in coastal regions. Globally at least 500 million people are highly dependent on coral reef ecosystems in one way or another (Hoegh-Guldberg, Pendleton and Kaup, 2019). Many people depend on coral reefs as an important nutrition source as reefs serve as nursing and feeding ground for many economically important fish and crustacean species (Hoegh-Guldberg, Pendleton and Kaup, 2019). Moreover, Coral reefs create underwater structures that can mitigate coast damage from tsunamis or floodings (Reguero et al., 2021). Coral reefs are also big tourist attractions. In Thailand alone reef adjacent and on reef tourism creates an annual revenue of ~US$2.4 billion (Spalding et al., 2017). The global economic value of coral reefs located in more than 100 jurisdictions is estimated to be worth trillions of US$ (i.e. Costanza et al. 2014; Reguero et al. 2021; Spalding et al. 2017).

Anthropogenic climate change increasingly threatens coral reefs (Hughes *et al.*, 2018). One major risk of global temperatures rising is the elevated threat of mass coral bleaching events. Hereby, as a response to intracellular stress the dinoflagellate symbionts are expelled from the coral and only the white host tissue remains on the skeleton. As these symbionts supply energy to the coral host through photosynthesis, bleached corals can become energy deficient. Consequently, bleached corals show reduced growth, reproduction and health, including reduced protection against diseases (Eakin, Sweatman and Brainard, 2019). If bleaching continues over an extended period of time corals are unable to keep up essential life functions and ultimately decease. Bleaching events have become more and more frequent in recent years and resulted in major losses of coral populations globally (Hughes *et al.*, 2018). Between 2014 and 2017 many regions suffered back to back bleaching events for the first time since recording (Eakin, Sweatman and Brainard, 2019). Furthermore, recovery of coral reefs is declining as reproductive success and recruitment are negatively affected by other anthropogenic stressors such as pollution (Richmond, Tisthammer and Spies, 2018).

According to the Intergovernmental Panel on Climate Change (IPCC) coral reefs are projected to decline by over 70% even if the goals of the Paris Agreement as an increase of 1.5°C until 2100 are reached (Bindoff *et al.*, 2019). Already at 2°C the expected decline increases to ~99%. Adaption might be able to delay such drastic loss of coral populations but will not be fast enough to prevent it under all but the lowest representative concentration pathway (RCP 2.6) modeled by the IPCC (Kleypas *et al.*, 2021).

Local extinctions of reef building corals would have devastating effects for the vast number of species and people that depend on them as well. However, it has become apparent, that the effects of global warming have progressed too far to preserve the majority of coral reefs (Kleypas *et al.*, 2021). Nevertheless, a focused protection effort on reefs with increased chances of surviving the challenges of future climate change, coupled with an increasing push to mitigate global warming could still lead to the existence of some healthy reefs in the future (Safaie *et al.*, 2018; Kleypas *et al.*, 2021). These reefs could essentially function as save refuges and origins for reef recolonizations. Coral reef sites that are routinely under the influence of internal waves (IW) have been proposed as such refuge candidates (Wyatt *et al.*, 2020).

Large Amplitude Internal Waves (LAIW) in the Andaman Sea

In contrast to surface waves internal waves travel along the pycnocline that separates the warm surface water from the cold deep water. At shallower waters along the continental shelf these waves interact with the underwater topography and break. Thereby, sub thermocline water that is generally cooler, more hypoxic, reduced in pH as well as enriched in nutrients is introduced into the surface layer (Vlasenko and Stashchuk, 2007). In some areas these waves have been shown to reach into shallow coral reef environments e.g. Florida Keys (Leichter *et al.*, 1996), outer Great Barrier Reef (Wolanski and Pickard, 1983), Dongsha Atoll (Fu *et al.*, 2012; Reid *et al.*, 2019) with measurable effects on reef temperature, oxygen, pH, and inorganic nutrients. While upwelling via Ekman transport shows some of the same effects on a bigger space and time scale, deep water introduction via internal waves is characterized by short, intense changes that occur repeatedly throughout the day (Reid *et al.*, 2019). Temperature changes from internal waves are largely invisible to sea surface temperature measurements by satellite as measurements are often not frequent enough, lack necessary resolution and above all only penetrate the top millimeter of the water column (Leichter, Helmuth and Fischer, 2006; Wyatt *et al.*, 2023).

In the Andaman Sea internal waves show extraordinary large amplitudes of 60m or higher (Osborne and Burch, 1980) and occur at high frequency with several large amplitude internal waves (LAIW) breaking per hour (Schmidt *et al.*, 2012). LAIW originate at the Nicobar island ark and travel in north-eastern direction towards the Thai coast (Osborne and Burch, 1980). When LAIW interact with the continental slope they transform into (internal) wave packages of typically 5 or 6 waves. Waves with larger amplitudes travel faster than smaller ones, which leads to waves in a wave package ordering themselves by their amplitude (Osborne and Burch, 1980). When these waves break, they create cold water pulses that wash over shallow near shore regions.

LAIW in the Andaman Sea show strong seasonality as they are affected by the annual cycle of southwest monsoon and northeast monsoon. During the northeast monsoon from January to May the pycnocline shoals and LAIW periodically reach shallow reefs and affect their environment. In contrast during the southwest monsoon from June to October the pycnocline is pushed deeper and less LAIW travel upslope (Wall *et al.*, 2012; Wall, Doering, *et al.*, 2023).

Due to their orientation the islands in the Andaman Sea function as natural barriers that shelter their eastern shores from LAIW effects while western shores are exposed to them. This leads to coral reefs in close proximity being exposed to drastically different environments. On exposed western reefs LAIW are a periodic disturbance factor leading to suppression in the development of a three-dimensional reef framework. Instead of a connected reef, isolated scattered coral colonies are found (Schmidt *et al.*, 2012; Wall *et al.*, 2012). Additionally, LAIW compress coral growth rates (Schmidt and Richter, 2013).

However, LAIW packages also provide many benefits to exposed coral reefs. The supplied deep water pulses lead to high thermal variability that can alleviate thermal stress during heat waves (Wall *et al.*, 2015; Schmidt *et al.*, 2016; Wyatt *et al.*, 2020). As a result coral reefs on LAIW exposed sites are more diverse, as they can harbor bleaching susceptible species that struggle to survive elsewhere (Schmidt *et al.*, 2012). Additionally, corals from exposed reefs have been shown to be more resilient than corals from sheltered reefs even when both are exposed to the same heat stress conditions (Buerger *et al.*, 2015; Wall, Doering, *et al.*, 2023). In fact the differential in heat resistance largely prevails even during the southwest monsoon where LAIW are absent (Wall, Doering, *et al.*, 2023). Consequently, there must be so far unknown intrinsic physiological differences that make corals from exposed sites more bleaching resistant in general. These could involve a shift in trophic strategy towards more heterotrophy, which is known to buffer against bleaching.

Corals show trophic variability

Commonly, healthy shallow water corals acquire the vast majority of their daily energy via photosynthates supplied by their dinoflagellate symbionts (here after just referred to as symbionts). However, corals are also able to supply large amounts via heterotrophic feeding to optimize their energy and essential nutrient acquisition (Muscatine *et al.*, 1984; Grottoli, Rodrigues and Palardy, 2006). The relative amount of autotrophy to heterotrophy is a dynamic spectrum and varies between and within coral species (Conti-Jerpe *et al.*, 2020; Sturaro *et al.*, 2021). In fact there is evidence of high trophic flexibility of conspecifics living only meters apart (Fox *et al.*, 2019).

Heterotrophic energy acquisition has a large impact on environmental stress resistance (Chapron *et al.*, 2022). More specifically, experimental evidence shows that feeding during high temperatures can

instantaneously alleviate bleaching risk (Tagliafico *et al.*, 2017; Huffmyer *et al.*, 2021) and prevent the photosystem within the symbionts from breaking down (Ferrier-Pagès *et al.*, 2010). The ability of a coral to supply itself with energy through heterotrophy also greatly enhances its recovery from bleaching events by maintaining its physiological status with less to no support from its symbionts (Grottoli, Rodrigues and Palardy, 2006). Furthermore, corals recovered from bleaching show increased heterotrophy more than 11 months later. While this might be indicative of a prolonged recovery phase it has also been hypothesized that this could indicate an acclimatization process, decreasing bleaching during the next heat event (Hughes and Grottoli, 2013). Additionally, a general trend can be observed of more heterotrophic coral species also being the more bleaching resistant species (Conti-Jerpe *et al.*, 2020).

In the Andaman Sea LAIW introduce deep water nutrients onto exposed western reefs. It has been shown that these nutrients fuel trophic networks and lead to higher mean daily particulate organic carbon and plankton mass fluxes (Roder *et al.*, 2010). If corals utilize these resources and increase their heterotrophic intake resulting in an overall shift in trophic strategy it could explain the higher bleaching resistance found in corals from LAIW exposed sites. Coral trophic strategy can be assessed by many ways. Recently novel approaches emerged utilizing stable isotopes and fatty acids to quantify relative heterotrophic and autotrophic input to the coral host.

Investigating coral trophic strategy via stable isotope analysis

Isotopic niche as a proxy for trophic niche can be evaluated via stable isotope analysis of carbon and nitrogen. Due to a process called trophic fractionation the heavier isotopes ^{15}N and ^{13}C are enriched relatively to the lighter isotopes ^{14}N and ^{12}C during each trophic step. This relative increase of ^{15}N to ^{14}N ($\delta^{15}N$) and ^{13}C to ^{12}C ($\delta^{13}C$) is fairly consistent with ~2-4‰ increase in $\delta^{15}N$ and ~0-1‰ increase in $\delta^{13}C$; therefore it is possible to infer the number of trophic steps between two organisms (DeNiro and Epstein, 1978; Minagawa and Wada, 1984; Peterson and Fry, 1987). While $\delta^{13}C$ is less reliable in identifying trophic position than $\delta^{15}N$, it is more consistent between predator and prey and can therefore be used to identify the source of dietary carbon, e.g. differentiation of benthic with pelagic sources (Fry and Sherr, 1989).

Coral host and symbiont tissue show similar values of $\delta^{13}C$ and $\delta^{15}N$ when corals are in a primarily autotrophic state. Heterotrophic input from the host leads to differences in $\delta^{13}C$ and $\delta^{15}N$ from host and symbiont getting larger as the consumed diet has a different isotopic signature than the photosynthates supplied by the symbiont (Muscatine, Porter and Kaplan, 1989; Nahon *et al.*, 2013). Therefore the differences in $\delta^{13}C$ and $\delta^{15}N$ of paired hosts and symbiont fractions ($\delta^{13}C_{H\text{-}S}$, $\delta^{15}N_{H\text{-}S}$) are

used to identify trophic decoupling of both symbiotic partners (Muscatine, Porter and Kaplan, 1989; Nahon *et al.*, 2013; Price *et al.*, 2021). A novel method by Conti Jerpe et al. (2020) extends upon this approach by investigating trophic strategy of corals by comparing the isotopic niche of their coral host and symbiont fractions utilizing SIBER analysis ("Stable isotope Bayesian Ellipses in R"). First $\delta^{15}N$ and $\delta^{13}C$ data of separated coral hosts and symbionts are plotted in an isotopic biplot and ellipses are drawn for each faction. The extend of overlap of coral host ellipses with the symbiont ellipses then indicates both partners utilizing the same resource pool and thus a lack of feeding from the coral host. The consequence is an increased reliance of the coral host on its symbionts for energy acquisition. Additionally, Conti Jerpe et al. found that overlap between coral host and symbiont isotopic niche was negatively correlated with bleaching resistance on a species level. This is further evidence that heterotrophy seems to increase bleaching resistance. (Conti-Jerpe *et al.*, 2020).

In addition to analyzing trophic strategy via SI analyses, a combination with other methods like fatty acid analysis might lead to a more robust assessment (Couturier *et al.*, 2020).

Fatty acids as health and trophic indicators

Fatty acids (FA) can be categorized by their degree of saturation: saturated fatty acids (SFA), monounsaturated fatty acids (MUFA) and polyunsaturated fatty acid (PUFA). SFA and MUFA are mainly prevalent in storage lipids while PUFA are integral in structural lipids and essential in cellular functions i.e. immune responses and signaling functions (Rocker *et al.*, 2019; Kim, Lee, *et al.*, 2021). Additionally, PUFA are crucial in coral reproduction mechanisms (Figueiredo *et al.*, 2012). While some higher trophic levels lack the necessary enzymes for de-novo PUFA synthetization, recent evidence showed that these are widespread in cnidaria including a large variety of tropical corals (Kabeya *et al.*, 2018). This must be considered when FA profiles are interpreted.

While studies often include single FA concentrations as well, using FA ratios instead has the advantage of sub-compositional coherence: Ratios stay the same regardless how many other FAs are included in the dataset, while relative concentration of single FAs change due to normalization. This means that two studies employing the same ratio can be compared even if they included different FAs in their overall dataset. (Graeve and Greenacre, 2020). FA ratios have been intensively used in other systems (e.g. zooplankton food web analysis) to understand trophic transfer and provide insight in energy acquisition for a long time (Bottino *et al.*, 1980; Graeve, Kattner and Hagen, 1994; Dalsgaard *et al.*, 2003). More recently these markers are tested in corals exploring relationships with trophic strategy and health status.

While some markers may be promising other seem to be more ambiguous (Kim, Baker, *et al.*, 2021). The differentiation of FA indicators in corals being influenced by health status or by feeding mode can be difficult, as feeding in itself improves health status (Tagliafico *et al.*, 2017; Veronica Z Radice *et al.*, 2019; Huffmyer *et al.*, 2021). For instance the ratio of eicosapentaenoic acid (EPA, C20:5n-3) to arachidonic acid (ARA, C20:4n-6) is used as a coral health marker (Rocker *et al.*, 2019; Safuan *et al.*, 2021; Zhang *et al.*, 2023). However, it could also be interpreted as a trophic marker, with EPA being a dominant FA in symbionts which can be transferred to coral hosts (Revel *et al.*, 2016; Kim, Lee, *et al.*, 2021) and ARA being negatively correlated with symbiont density and thought to originate from prey items (Seemann *et al.*, 2013; Rocker *et al.*, 2019; Kim, Lee, *et al.*, 2021). The assessment of trophic strategy through fatty acid profiles is further complicated by the ability of both hosts and symbionts to obtain fatty acids by multiple ways: via de novo synthetization, via transport from the symbiotic partner and via the hosts diet (Revel *et al.*, 2016; Kim, Lee, *et al.*, 2021). As an example another ratio including EPA, the ratio of EPA : DHA (Docosahexaenoic acid, C22:6n-3), has been suggested as a marker for reliance on autotrophic input for corals. EPA, as stated above is a major component in symbionts and DHA is conserved in the food web and has been used to indicate carnivory (Graeve, Kattner and Hagen, 1994; Rocker *et al.*, 2019). However, the ability of the symbiont to supply the coral host with either DHA, EPA or both undermines coral trophic strategy estimation through this marker if supply capabilities of the symbiont are not considered as well (Revel *et al.*, 2016; Kim, Lee, *et al.*, 2021). Nevertheless, a multitude of fatty acid trophic markers, including EPA : DHA, can be successfully applied in coral systems when limitations are considered.

Using fatty acid analytics for coral health status and trophic strategy assessment remains a relatively novel and evolving field. In recent years, there has been a surge in coral fatty acid research indicating its considerable potential for the future. In this thesis a range of FA ratios will be used to identify differences in tropic strategy and health status between corals from LAIW exposed and LAIW sheltered sites.

Study species *Porites lutea* and *Pocillopora verrucosa*

Two sclearactinian corals, *Porites lutea* and *Pocillopora verrucosa,* were used as study species in this thesis. The two species show differing growth forms with *P. lutea* having a massive morphology while *P. verrucosa* displays branching morphology. *P. verrucosa* is sometimes described as an effective heterotroph (Veronica Z. Radice *et al.*, 2019) but some studies also found limitations in their ability to supply energy via heterotrophy (Séré *et al.*, 2010; Ziegler *et al.*, 2014). *P. lutea* shows high phenotypic plasticity and is commonly characterized as a mixotroph (Sawall *et al.*, 2014; Conti-Jerpe *et al.*, 2020). In the Andaman Sea *Porites spp*. are the dominate coral species on many LAIW sheltered reefs but are less dominant in LAIW exposed reefs (Brown, 2007; Schmidt *et al.*, 2012). In contrast *Pocillopora spp*. are highly abundant in LAIW exposed reefs (Brown, 2007; Gibson, Atkinson and Gordon, 2007). A recent study compared heat stress in *P. verrucosa* and *P. lutea* from Patong Bay, Thailand. They found *P. verrucosa* to be more sensitive than *P. lutea*, in fact *P. verrucosa* completely bleached after 6 days at 2°C while *P. lutea* only showed partial reduction in symbiont densities and photosynthetic efficiency after 9 days (Jain *et al.*, 2023). Importantly, both species show increased bleaching resistance with LAIW exposure in their life history (Buerger *et al.*, 2015; Wall, Doering, *et al.*, 2023). The differences in physiological and morphological traits, as well as the differences in relative abundance on LAIW exposed reefs make these species suitable candidates to investigate the effects of LAIW on trophic strategy. Given that both species have enhanced bleaching resistance at LAIW-exposed sites, evaluating their trophic strategies could reveal whether this resilience stems from increased heterotrophy.

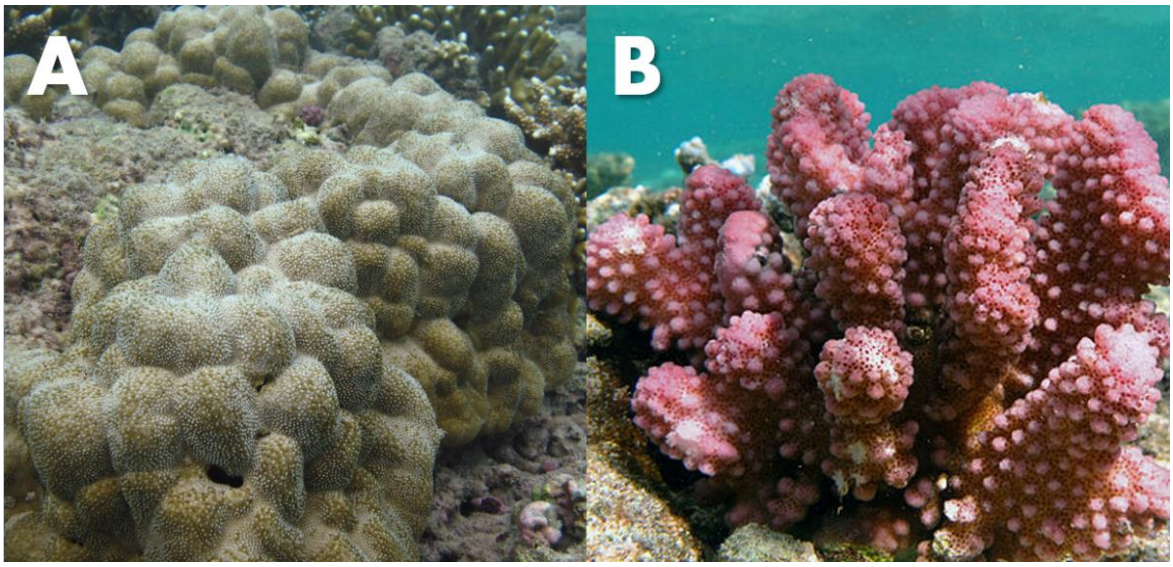

Figure 1: Study species used in this thesis:
***A:** Porites lutea (Picture: Michel Claereboudt; coralsoftheworld.org)*
***B:** Pocillopora verrucosa (Picture: Philippe Bourjon; wikimedia.org)*

Aim of this thesis

In this thesis I aim to take advantage of adjacent but distinct reef habitats to disentangle the role of trophic strategy as the driver for improved bleaching resistance of LAIW exposed corals. Additionally, differences in coral health markers due to LAIW exposure will be assessed.

LAIW induced deep water nutrients and the following increase in POC and plankton flux might enhance corals heterotrophic energy input and thus drive bleaching resistance observed in corals from LAIW exposed reefs. If corals utilize this input, it should result in differences in fatty acid and stable isotope profiles of separated host and symbiont fractions between LAIW exposed and LAIW sheltered corals. The resulting pattern allow the answer of the following research questions:

RQ_A: Does upwelling in LAIW sites result in shifts in trophic strategy within the coral species *Porites lutea* and *Pocillopora verrucosa*, explaining the higher bleaching resistance of LAIW exposed corals?

> $H0_A$: FA and SI heterotrophy markers will show no significant differences between corals from LAIW exposed and LAIW sheltered sites, indicating the same trophic strategy on a population level.
>
> $H1_A$: FA and SI heterotrophy markers will be significantly higher in corals from LAIW exposed sites compared to corals from LAIW sheltered sites showing a shift in trophic strategy.

RQ_B: Does upwelling in LAIW sites result in in a better health status within the coral species *Porites lutea* and *Pocillopora verrucosa*?

> $H0_B$: FA health markers and biomass per surface area will show no difference between corals from LAIW exposed and LAIW sheltered sites.
>
> $H1_B$: FA health markers and biomass per surface area will be significantly higher in corals from LAIW exposed sites compared to corals from LAIW sheltered sites.

Material and methods

Coral Sampling

Coral fragments of the species *Porites lutea* and *Pocillopora verrucosa* originated from LAIW exposed western and LAIW sheltered eastern reefs of the islands Racha and Miang in the Andaman Sea (Figure 2). Colleagues from the Phuket Marine Biology Station (PMBC) took the samples during peak LAIW season in March/April of 2018. Right after sample collection whole fragments were snap frozen in liquid nitrogen and stored at -80°C until processing. The aim was to analyze 16 holobionts per species, island, and site. However, not all populations at the sampling sites recovered from the massive bleaching event in 2010. That limited the sampling of both species with the lowest number of holobionts sampled being eight *Porites* at Miangs eastern site. Additionally, some samples were too small to allow the full set of host and symbiont trait measurements, and some samples were lost during laboratory work. Final sample number per group and analyses can be found in Supplement Table 2.

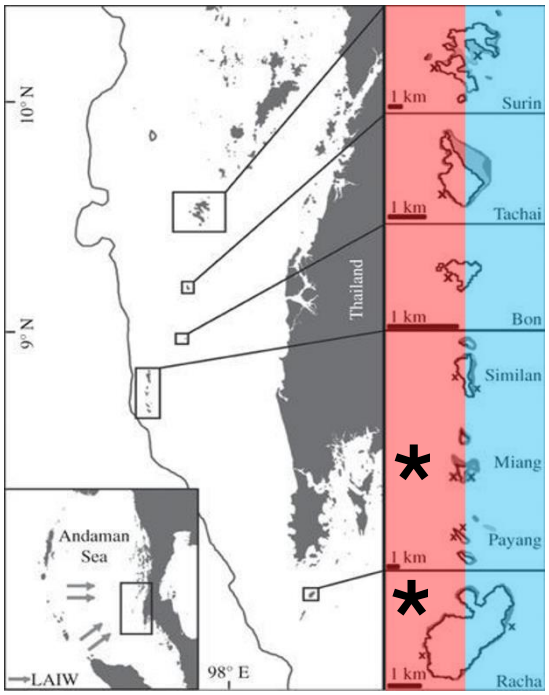

Figure 2: Islands in the Andaman Sea with western sites exposed to large amplitude internal waves (LAIW) in red and eastern LAIW sheltered sites in blue. The study sites Miang and Racha are marked with an asterisk. Travel direction and origin of LAIW at the Nicobar Island ark is shown at the bottom left.

Sample processing

The various analyses included in this thesis required prior coral holobiont tissue separation from the calcium carbonate skeleton and subsequently, symbiont cell isolation from coral host tissue. The procedure followed Price et al. (Price *et al.*, 2020) but was slightly adapted for the smaller fragments used in this study.

Tissue was separated from the skeleton by airbrushing the coral nubbins with a pipette tip on a hose connected to a lab air pressure valve. Tissue was collected in 50ml falcon tubes. While airbrushing droplets of milliQ water were occasionally added to increase airbrushing efficiency and guide tissue into the falcon tube. Skeletal architecture allowed for easy tissue separation in *Pocillopora* samples,

but not in *Porites* samples. Therefore, airbrushing process was defined as being complete in *Porites* when similarly light brown nubbins remained. Falcon tubes containing the coral slurry were immediately stored at -80°C until further processing. The remaining skeleton was subsequently used for surface area estimation.

For host-symbiont tissue separation coral holobiont slurry was defrosted on ice and homogenized for 60 seconds using an "Ultra-thurrax® IKA® T18 basic". Afterwards, tissue slurries were centrifuged at 1700g for 5 minutes and the supernatant containing the host was transferred to a 15 ml falcon tube. The remaining pellet was resuspended in artificial salt water (~30 PSU) and centrifuged again at 600g for 5 minutes. The resulting supernatant was added to the host fraction. This step was repeated once again to make sure no coral tissue remained in the symbiont pellet. Thereafter, host fraction was centrifuged at 2000g and supernatant was moved to a new 15ml falcon tube to remove a possible contamination with symbiont cells. Symbiont pellets were resuspended in artificial sea water for a total volume of 10ml. Falcon tubes containing host fraction were toped up with milliQ to a total of 10ml as well, making whole sample calculations for each analysis straight forward.

Separated host and symbiont fractions were aliquoted for biomass, stable isotope, and fatty acid analyses. Glass vials were used for fatty acid aliquots (per Couturier *et al.,* 2020) while stable isotope and biomass fractions were stored in 15ml falcon tubes. Residual skeleton had to be removed from the stable isotope aliquots as the present carbon would have influenced $\delta^{13}C$ measurements. This was achieved by adding drops of 10% hydrochloric acid (HCl) which reacts with calcium carbonate ($CaCO_3$) creating calcium chloride ($CaCl_2$), water and carbon dioxide (CO_2). Therefore, it can be assured that no more skeleton carbon is present in the sample when no more carbon dioxide bubbles are formed after HCl addition. All aliquots were again stored at -80°C before further analyses.

Surface area of coral nubbins was approximated via geometrical shapes, which has been shown to be more accurate than surface area estimation via planar photography or wax coating (Naumann *et al.*, 2009). In cases where nubbins showed growth forms vastly different from a single geometrical shape or displayed large differences in dimensions at several parts a combination of multiple shapes was used to achieve a more accurate approximation. For most samples spherical caps and cylinders with and without bottom and top were used but some unusual growth forms had to be approximated via the addition of triangles, rectangles, and circles. Geometric dimensions were assessed by taking the average of multiple measurements with an electronic caliper.

Sample analysis of separated host and symbiont fractions

Ash free dry weight:

Prior to ash free dry weight (AFDW) measurements small aluminum pans (~1cm height; ~3cm diameter) were prebaked at 600°C overnight to remove any impurities and water in them. Pans were then labeled and weighted on a microscale (accurate to 0.1µg). Depending on slurry color a sub sample of 0.5 or 1ml of coral/symbiont slurry was added. Pans were then left in a drying oven at 60°C for ~72h and weighed again to determine the tissue dry weight of each subsample. Afterwards, pans were baked at 900°C for 13h to remove all organic carbon and reweighed to quantify AFDW. AFDW of the entire fragments host or symbiont fraction was then calculated by dividing the total AFDW of the subsample by the used volume and multiplying it by the full sample volume (10ml). AFDW was then normalized to surface area for group comparisons.

Stable isotope analysis

Sample preparation for stable isotope analysis (SIA) was done via a modified protocol from the procedures described in Price *et al.*, 2020: Between 2 and 3ml of the whole sample slurry was used as subsample. SIA of carbon ($\delta^{13}C$) and nitrogen ($\delta^{15}N$) required filtering the subsample on prebaked glass filters (0.07µm, Whatman™, GF/F) and freeze drying ("CHRIST freeze dryer Alpha 1-4 LSC") of the filter for 24h. Between 5µg and 120µg of carbon and between 2.5µg and 12µg of nitrogen was required. Filter color gave initial information about the filtered biomass, then either the entire filter or portions of the filter were loaded into a tin capsule (5 x 9 mm, "IVA Analysetechnik GmbH & CO KG").

SIA of carbon and nitrogen was done via the methods described in Hansen, Burmeister and Sommer, 2009: Measurements were performed by a high sensitivity elemental analyzer (CE INSTRUMENTS EA1110) coupled with an isotope mass spectrometer (DeltaPlus Advantage, Thermo Fisher Scientific). Acetanilide (C_8H_9NO) served as an external standard and was measured periodically after 6 samples to calibrate the measurements. In cases where carbon or nitrogen weights fell outside the boundaries of the calibration curve, SI sample preparation and SIA was repeated.

Fatty acid profiling

Fatty acid profiling was done using a modified version of the methods described in Bligh and Dyer, 1959 and Folch *et al.*, 1957. In this method all fatty acids (FA) from all lipids are extracted and esterified before quantification of fatty acids methyl esters (FAME) via gas chromatography. The potential impact of small volumes of sample being lost during the extensive laboratory protocol is minimized by incorporating internal standards of known concentrations prior to the first step: We can assume that if

small volumes of FA are lost at any step (e.g. leftover droplets), internal standard is lost at a similar rate. As all FA concentrations are calculated as their relative peak area compared to the internal standards peak area the calculated concentrations stay the same.

The required volume for fatty acid analysis is quite flexible and was approximated through prior testing on coral host and symbiont fractions not included in this thesis dataset. Depending on surface area the subsample for FA analysis contained 2-4ml of the total coral host or symbiont slurry. Before FA could be extracted the subsample had to be freeze dried ("CHRIST freeze dryer Alpha 1-4 LSC"). FA extraction was done by adding 3ml of a 1:1:1 mixture of chloroform ($CHCl_3$), dichloromethane (CH_2Cl_2) and methanol (CH_3OH) to the freeze-dried tissue. 100µl of the internal standards C19:0 (as fatty acid methyl ester; c=20.603ng/µl) and C21:0 (as fatty acid, c=30.103ng/µl) were added to each sample and then left at -20°C for an extraction period of 24h.

Afterwards samples were transferred from glass vials to separation flasks by washing the glass vials twice with 1ml of 1:1:1 extraction solvent solution. Subsequently, 2.25ml of 1M potassium chloride solution (KCl) was added to separate two phases: an upper phase containing mostly methanol and proteins and a lower phase containing mostly chloroform, dichloromethane, and lipids. The latter was transferred to a pear-shaped flask. The upper layer was then washed twice with dichloromethane and the resulting lower layer was added to the pear-shaped flask to add any remaining lipids from the methanol layer. Afterwards, residual water in the lipid phase was removed by adding a small amount of sodium sulfate (Na_2SO_4) to the pear-shaped flask. The extract was then carefully moved to a centrifuge vial while making sure no Na_2SO_4 was transferred. ~1ml of CH_2CL_2 was added to the flask and then transferred to the centrifuge vial twice to make sure all lipids were moved. Extracts were cooled at -20°C for 1 hour before being reduced to total dryness in a rotary evaporator ("Heidolph Laborota 4000 efficient"). Subsequently, the sample was redissolved in 100µl $CHCl_3$ and transferred to a glass cocoon. The glass cocoons were self-made by sealing the top of a 2ml glass pipette with a blow torch. To ensure the transfer of all FAs 100µl of $CHCL_3$ was added two more times to the centrifuge vial and then added to the glass cocoon. Extracts were once again dried by removing $CHCl_3$ in the rotary evaporator. Afterwards 100µl of Toluene ($C_6H_5CH_3$) and 200µl of 1% sulfuric acid (H_2SO_4) in methanol (CH_3OH) were added on the dried extract for the esterification step. Cocoons were flushed with nitrogen gas, closed by burning the tip with a blow torch and left in an oven set to 50°C for at least 12h. Here, the methanol is necessary as a donor of the methyl group to esterify FAs in a reaction with H_2SO_4 and nitrogen is added to create an anoxic environment necessary for the reaction. Similarly, the high temperature also accelerates the reaction, but must be kept below the boiling point of methanol at 65°C (Zhen and Wang, 2015).

After the esterification step FAMEs had to be reextracted. First 100µl of 5% sodium chloride in deionized water was added to highlight the phase separation. Then FAME were extracted by adding three portions of 100µl n-hexane (C_6H_{14}) and transferring the top layer containing FAME into a new glass cocoon. Afterwards, the extract was dried in the rotary evaporator one last time. Finally, 100µl of n-hexane was added to the extract and transferred into a 2ml glass GC-autosampler-vial with an inlay for low volumes. In addition to the coral samples, a blank sample was added per day only containing internal standards to assess potential contamination throughout sample preparation.

1µl of the final extract was analyzed by a gas chromatograph ("Thermo ELECTRON CORPORATION Trace GC Ultra") coupled with an autoanalyzer ("Thermo SCIENTIFIC AS 3000") using hydrogen as carrier gas. Additionally, two external standards, "SUPELCO® 37 component FAME mix" and a bacterial fatty acid methyl ester mix (BAME) were measured three times and one time respectively before each set of samples. The identification of individual FA peaks in the chromatograms was facilitated by comparing their retention times to those of the external standards. Weight in ng of individual FAs was derived by their peak area compared to the peak area of the internal standard C19. Weight of the internal standard C21 was calculated and compared to the known weight added to the sample to calculate esterification efficiency. FA weights were then multiplied by the esterification efficiency resulting in the theoretical weight if 100% of FAs were esterified. Individual FA weights of the blank samples were then subtracted from the corresponding FAs in the samples prepared on the same lab day. In case where this resulted in a slight negative weight for single FAs, the concentration for these FAs was set to zero instead. Finally, concentrations were normalized to surface area (ng FA*mm^{-2}) and relative concentrations in percent single FAs of total FAs were calculated.

Data analyses and statistics:

All statistical and data analyses were performed in R version 4.2.0 (R Core Team, 2022). Data organization and visualization was done with the help of the packages "tidyverse" (Wickham *et al.*, 2019) and "ggplot2" (Wickham, 2016) respectively.

Stable isotope analyses

The differences from host and symbiont $\delta^{13}C$ values ($\delta^{13}C_{H\text{-}S}$) and $\delta^{15}N$ values ($\delta^{15}N_{H\text{-}S}$) were calculated for each coral holobiont. Additionally overlap of isotopic niche was analyzed via the "SIBER: Stable Isotope Bayesian Ellipses in R" package (Jackson and Parnell, 2023) as per Conti-Jerpe et al. 2020. Standard ellipse areas corrected for sample size (SEAc) containing 40% and 95% of the data were drawn reciprocally to minimize the effect of type 1 and type 2 errors respectively (Conti-Jerpe *et al.*, 2021;

Thibault, Lorrain and Houlbrèque, 2021). In other words, drawing 40% SEAc ellipses increases the chance of the plots showing distinct isotopic niches that do not exist, while drawing 95% ellipses risks masking distinct isotopic niches. As the sample size per species, island, and site was below the recommended sample size for SIBER analysis (n>30, (Syväranta *et al.*, 2013)) data from both islands was pooled to compare overall isotopic niche overlap from LAIW exposed sites to sheltered sites. However, due to limited availability of samples the pooled count was still below 30 (Supplement Table 2). Subsequently, Euclidean distances between the centroids (bivariate means of $\delta^{13}C$ and $\delta^{15}N$) were calculated. Significant differences in the relative placement of each species host and symbiont fraction in isotopic space was determined by applying residual permeation procedure (RPP) and Hotelling's T^2 test utilizing the R script from Turner et al. (Turner, Collyer and Krabbenhoft, 2010).

Fatty acid analyses

Relationship between full fatty acid profiles, LAIW exposure, Islands, coral species and symbiotic partners was first visualized in a log ratio analysis (LRA) plot utilizing the R package "EasyCODA" (Greenacre, 2018). To avoid generating infinite values when calculating log ratios, zeros in absolute values for individual FA were substituted with half the minimum quantity found across all other samples. This method is justifiable, as an amount of zero ng of a given FA is not a true zero but an amount beneath the detection limit of the gas chromatograph.

Ratios of FAs with known physiological relevance were calculated (Table 1). Putative health markers included the amount of PUFA and the fatty acid ratios EPA : ARA and n-3 PUFA to n-6 PUFA. PUFA serve important roles in organism functioning and low levels might indicate an unhealthy or stressed coral. (Bachok, Mfilinge and Tsuchiya, 2006; Revel *et al.*, 2016). The ratio of EPA : ARA can be employed as an indicator for a coral health status as well (Rocker *et al.*, 2019; Safuan *et al.*, 2021; Zhang *et al.*, 2023). While ARA is required for pro-inflammatory processes and water transport across cell membranes, EPA plays a major role in anti-inflammation. High concentrations of ARA without equally high concentrations of EPA can therefore lead to inflammation becoming uncontrollable (Simopoulos, 2008). The ratio of n-3 to n-6 as a health indicator is closely linked to the EPA : ARA ratio but takes into consideration that pathways for both EPA and ARA synthetization exist within the corals. N-3 PUFAs are substrates for EPA, while n-6 PUFAs are substrates for ARA. As both pathways utilize the same enzymes competition takes place where the pathway with the higher amount of substrate dominates (Kim, Lee, *et al.*, 2021). In addition to being a precursor for EPA, n-3 PUFA concentrations enhance electron transfer and are linked to improved growth and stress resistance. Therefore a higher n-3 to n-6 ratio in a coral host is indicative of a higher health status (Rocker *et al.*, 2019). Results from a study analyzing

Table 1: Overview of fatty acid markers employed in this thesis

	Ratio	Marker for	Fatty acids	Reference
Health Marker:	EPA : ARA	Pro-inflammatory vs Anti-inflammatory	C20:5n-3 / C20:4n-6	Rocker *et al.,* 2019; Safuan *et al.,* 2021; Zhang *et al.,* 2023
	Sum PUFA	Health status (general organism functioning)	Sum of all PUFA*****	Bachok *et al.,* 2006; Revel *et al.,* 2016
	PUFA n-3 : PUFA n-6	Growth potential, stress resistance, enhanced electron transfer, inflammation control	Sum PUFA n-3* / sum PUFA n-6*****	Rocker *et al.,* 2019 Safuan *et al.,* 2021 Kim, Lee, *et al.,* 2021
Trophic marker:	EPA : DHA	Autotrophy	C20:5n-3 : C22:6n-3	Rocker *et al.,* 2019 Kim, Lee, *et al.,* 2021 (Legezynska *et al.* 2012)
	Animal derived : Photosynthesis derived	Heterotrophy	Animal derived: C18:1n9+C20:1n-9+ C22:1n-11 Photosynthesis derived: C16:1n-7+C18:1n-7 (Dataset in this thesis is missing C22:1n-11)	Radice *et al.,* 2019 Imbs *et al.,* 2010
	18:1n-9 : 18:1n-7	Carnivorous diet	18:1n-9 : 18:1n-7	Graeve *et al.,* 1997; Legezynska *et al,* 2012 Radice et al., 2019
	Long chain MUFA (LC-MUFA)	Feeding on herbivorous copepods	Sum of C20:1 FAs and C22:1 FAs (n-7, n-9, n-11) (In this thesis only n-9 MUFAs included)	Radice *et al.,* 2019; Wall, Beck, *et al.,* 2023 (Brett *et al.,* 2009)
	PUFA : SFA	Recent feeding, carnivorous diet	Sum PUFA : Sum SFA*****	Tolosa *et al.,* 2011; Kim, Baker, *et al.,* 2021; Kim, Lee, *et al.,* 2021
	Total fatty acids	Heterotrophy	Sum of all fatty acid	Treignier *et al.,* 2008 Tolosa *et al.*, 2011; Kim, Baker, *et al.*, 2021

*See Supplement Table 1 for a list of all fatty acids included in this thesis dataset

coral FA profiles under eutrophication supports this interpretation as corals exposed to low water quality had lower n-3 : n-6 PUFA ratios (Kim, Lee, *et al.*, 2021).

A variety of trophic markers were analyzed in this thesis as well (Table 1). The reasoning and background behind these markers being related to trophic strategy are explained as follows: The amount of long chain MUFA (LC-MUFA), consisting of C20:1 FAs and C22:1 FAs, has been applied as a marker in corals for potential feeding on herbivorous marine copepods as they harbor elevated concentrations of LC-MUFAs (Brett, Müller-Navarra and Persson, 2009; Veronica Z Radice *et al.*, 2019; Wall, Beck, *et al.*, 2023). As mentioned the ratio of EPA : DHA, has been suggested as a marker for reliance on autotrophic input for corals, as EPA is a dominant FA in symbionts which gets transferred to

coral hosts and DHA is conserved in the food web used to indicate carnivory (Graeve, Kattner and Hagen, 1994; Rocker *et al.*, 2019). Additionally, the relative amount of PUFA compared to SFA has recently been introduced as an indicator for coral carnivory (Tolosa *et al.*, 2011), as well as an indicator of recent feeding (Kim, Baker, *et al.*, 2021; Kim, Lee, *et al.*, 2021). The fatty acids C18:1n-9, C20:1n-9 and C22:1n-11 are thought to be markers for heterotrophy as well (Veronica Z Radice *et al.*, 2019). In contrast to that the fatty acids C16:1n-7 and C18:1n-7 are lower in coral host fractions than in coral symbiont fractions and have been suggested as markers for photosynthesis (Imbs *et al.*, 2010). Therefore the ratio of these fatty acids termed animal-derived FA to photosynthetically-derived FA has been used to evaluate trophic strategy of corals on a species level (Veronica Z Radice *et al.*, 2019; Wall, Beck, *et al.*, 2023). Related to this is the marker of 18:1n-9 to 18:1n-7. This ratio has been employed to indicate relative carnivory compared to herbivory in copepods (Graeve, Kattner and Piepenburg, 1997; Legezynska, Kedra and Walkusz, 2012) and has also been applied in corals as C18:1n-7 is likely transferred from the symbiont to the host (Veronica Z Radice *et al.*, 2019). Furthermore, heterotrophy has also been found to enhance the accumulation of lipids in general, therefore the total amount of FA was also used as a heterotrophy marker (Treignier *et al.*, 2008; Tolosa *et al.*, 2011; Kim, Baker, *et al.*, 2021).

While all the mentioned markers are used to indicate health status and trophic position by analyzing the coral host fraction, symbiont fractions FA ratios were also analyzed to show a complete picture and investigate possible FA transfer to and from the host.

Statistical analyses

Two-factorial ANOVAs with the factors “Site” and “Island” were fitted for AFDW and all FA markers, separate for each species and separate for host and symbiont fractions. To deal with the unbalanced study design categorical variables were treated using sum contrasts (Al-Sarraj and Forkman, 2023) and sums of squares were set to type three using the r package “car” (Fox and Weisberg, 2019). Levene’s test along with inspection of variance plots was utilized to assure homoscedasticity in each model’s data.

Normality of model residuals was assessed via quantile-quantile plots. Where ANOVA models showed non-normal residuals generalized linear models (GLM) with inverse gaussian or gamma distribution families were fitted instead. GLMs fit was analyzed by inspecting simulated residuals of the fitted model with the R package “DHARMa” (Hartig, 2022). Where both GLMs led to a good model fit, final model was chosen based on Akaike information criterion (AIC). Post hoc pairwise comparison was done via estimated marginal means (EMM) with Tukey Honest Significant Difference (HSD) correction with the R package “emmeans” (Lenth, 2022).

Furthermore, Cohen's d effect size was calculated for differences in FA trophic and health markers on eastern and western sites within islands. Calculation of Cohen's d was done with help of the R package "effsize" (Torchiano, 2020). Cohen's d normalizes the mean differences of two groups by their combined standard deviation. A heatmap was then created to get an overview of the effect sizes of all FA markers.

Results

Ash free dry weight per surface area

Biomass was measured for isolated coral host and symbiont tissue (Figure 3). *Porites* host AFDM per surface area was higher in corals from western LAIW exposed sites on both islands, however only the overall difference from west to east was significant (GLM, p=0.047, Supplement Table 4). Conversely, *Porites* symbionts showed the opposite relationship with island site. On both Racha and Miang *Porites* symbiont biomass per surface area was higher in corals from the eastern LAIW sheltered reefs. The effect of site per islands was not large enough to be detected in the post hoc test, but the overall effect of site was found to be significant (GLM, p=0.028, Supplement Table 4).

Pocillopora host biomass per surface area was lower on LAIW exposed sites on both islands but with a much larger effect on Miang. Measurements from the eastern site of Miang also had much higher variance then all other *Pocillopora* host sample groups. A similar pattern was observed for *Pocillopora* symbionts, with biomass and variance being higher on Miangs sheltered site than on its exposed western site (non-significant, EMM, p-value=0.371, Supplement Table 5). In contrast, the measurements showed no difference in symbiont biomass for Rachas eastern and western site. For *Pocillopora* neither site nor island nor the interaction of both was significant for either host or symbiont biomass per surface area. Nevertheless, overall LAIW sheltered *Pocillopora* host show higher AFDM per surface area than LAIW exposed hosts that should not be ignored (GLM, p=0.072, Supplement Table 4).

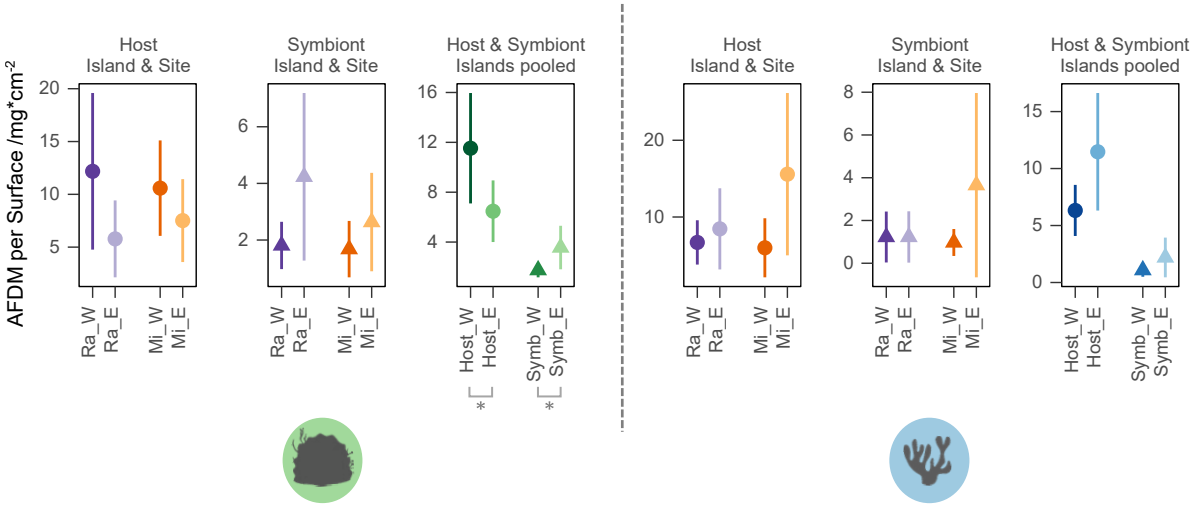

*Figure 3: Mean + 95% confidence interval from ash free dry mass per surface area measurements (mg*cm-2) of separated coral host and symbiodinium of Porites (left) and Pocillopora (right) from LAIW exposed western sites (W) and LAIW sheltered eastern sites (E) of the islands Racha (Ra) and Miang (Mi). Significant differences (p <0.001***, < 0.01**, <0.05*) from generalized linear models and post hoc estimated marginal means with Tukey HSD correction.*

Stable Isotope analyses

Mean values of raw isotope data $\delta^{13}C$ and $\delta^{15}N$ for each species symbiont and host fraction are stated in Supplement Table 2. The raw data was used to conduct SIBER analysis and calculate differences in host to symbiont isotopic signatures ($\delta^{13}C_{H\text{-}S}$ and $\delta^{15}N_{H\text{-}S}$; also found in Supplement Table 2).

$\delta^{13}C_{H\text{-}S}$ of *Porites* was very similar for the LAIW exposed western and the LAIW sheltered eastern site on Racha with 1.23 ± 1.4‰ and 1.31 ± 1.98‰ respectively. On Miang *Porites* showed a larger difference between western and eastern sites at 0.19 ± 0.39‰ and 0.77 ± 0.51‰ respectively (Figure 4a). $\delta^{13}C_{H\text{-}S}$ of both islands together cumulated to 0.83 ± 1.22‰ on LAIW exposed western sites compared to 1.09 ± 1.56‰ on LAIW sheltered eastern sites (Figure 4b).

$\delta^{15}N_{H\text{-}S}$ had much lower variance within sample groups, with standard deviations ranging from ±0.24‰ to ±0.93‰ across all sample groups. *Porites* on western and eastern sites were similar to another within both islands, but $\delta^{15}N_{H\text{-}S}$ on Miang was consistently higher with 0.71 ± 0.24‰ west and 0.63 ± 0.44‰ east, compared to Racha with levels of 0.26± 0.72‰ west and 0.23 ± 0.93‰ east (Figure 4e). Consequently $\delta^{15}N_{H\text{-}S}$ of both islands pooled did not show a strong difference with 0.39± 0.78‰ on western sites and 0.43 ± 0.61‰ on eastern sites (Figure 4f).

Pocillopora showed large variances in $\delta^{13}C_{H\text{-}S}$ on eastern island sites with values of 0.43 ± 2.34‰ on Racha and 1.08 ± 1.02‰ on Miang. Racha western sites mean $\delta^{13}C_{H\text{-}S}$ was quite similar to Racha east at 0.49 ± 0.53‰ while $\delta^{13}C_{H\text{-}S}$ on Miangs western site was lower than its eastern site at -0.06 ± 0.36‰

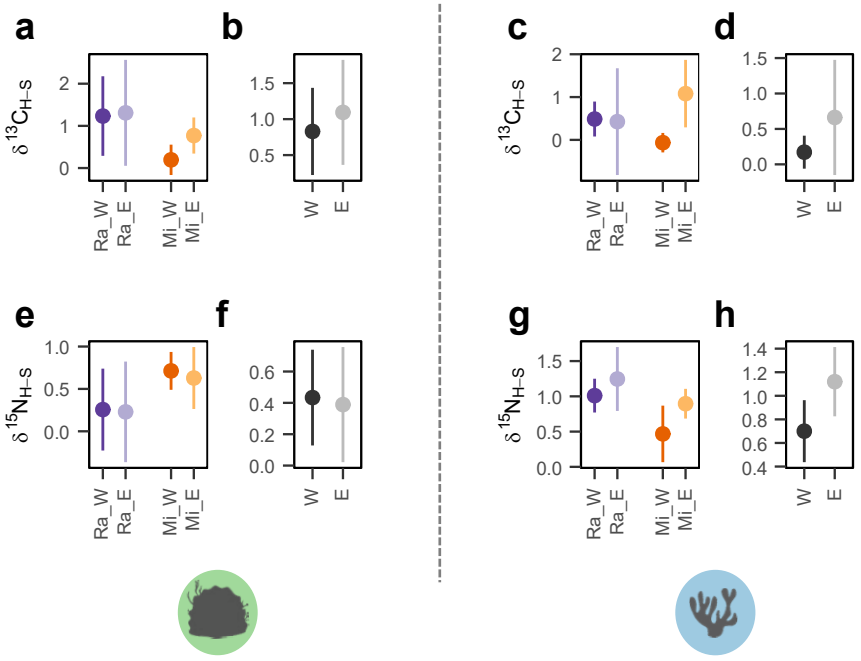

Figure 4: Differences in δ13C and δ15N of host and symbiont fractions. Porites (left) and Pocillopora (right). Coral originated from LAIW exposed western sites (W) and LAIW sheltered eastern sites (E) of the islands Racha (Ra) and Miang (Mi) in the Andaman Sea. (a) and (c) $\delta 13C_{H\text{-}S}$ per island and site. (b) and (d) $\delta 13C_{H\text{-}S}$ of both islands pooled. (e) and (g) $\delta 15N_{H\text{-}S}$ per island and site (f) and (h) $\delta 15N_{H\text{-}S}$ of both islands pooled. No statistical analysis was conducted.

(Figure 4c). The differences on Miang facilitated differences in $\delta^{13}C_{H\text{-}S}$ for both islands pooled at 0.66 ± 1.97‰ on eastern Sites and 0.17 ± 0.51‰ on western sites (Figure 4d).

Pocillopora had slightly but consistently higher values of $\delta^{15}N_{H\text{-}S}$ on eastern island sites. The eastern site of Racha had the highest $\delta^{15}N_{H\text{-}S}$ of all sample groups with 1.25 ± 0.85‰. Racha western site was not as high with 1.01 ± 0.31‰. *Pocillopora* on Miang had lower $\delta^{15}N_{H\text{-}S}$ than Racha with 0.47 ± 0.63‰ on its western Site and 0.90± 0.27‰ on its eastern site (Figure 4g). The higher $\delta^{15}N_{H\text{-}S}$ values of *Pocillopora* on both islands eastern sites cumulated to a higher overall $\delta^{15}N_{H\text{-}S}$ on eastern sites with 1.12 ± 0.71‰ compared to overall western sites with 0.70 ± 0.58‰ (Figure 4h).

SIBER analysis was conducted per species and site with data of both islands pooled. 95% maximum likelihood standard ellipses corrected for sample size (SEAc) were drawn for each sampling groups host and symbiont fraction (Figure 5). *Pocillopora* showed a near equal SEAc overlap on both sites with 53% on LAIW sheltered eastern sites and 54% overlap on LAIW exposed western sites. *Porites* SEAc overlap was larger than the overlap of *Pocillopora* SEAc on both island sites. SEAc of *Porites* on eastern sites had an overlap of 76% while the western sites showed a complete 100% overlap of the host SEAc. This suggests an increased reliance on autotrophy on western sites. Interestingly, Hotelling T^2 test and RPP reveal that *Porites* from eastern sites are the only sample group across both species where host and symbiont do not occupy a significantly different place in isotopic space (Table 2). Size of SEAc across host and symbiont fractions was quite consistent within each species, but west *Porites* host SEAc was much smaller than other *Porites* SEAc and *Pocillopora* symbiont SEAc from eastern samples was larger than other *Pocillopora* SEAc (Figure 6). SIBER analysis was also performed with 40% SEAc and followed the same trends as the analysis with 95% SEAc ellipses (Supplement Figure 1)

Table 2: Results of residual permeation procedures (RPP) and Hotelling T^2 test to identify significant differences in isotopic niche placement of coral host and their symbionts. Data originates from the islands Racha and Miang in the Andaman Sea. Western island sites are exposed to large amplitude internal waves (LAIW) while eastern sites are sheltered.

Species	Site	Euclidean distance host and symbiont centroids (‰)	RPP *p*	Hotelling T^2	Hotelling F	Hotelling *p*
Pocillopora	East (LAIW-)	1.30	**<0.001**	75.77	35.61	**<0.001**
	West (LAIW+)	0.72	**0.028**	35.52	16.49	**<0.001**
Porites	East (LAIW-)	1.16	0.083	3.79	1.75	0.171
	West (LAIW+)	1.07	**0.011**	9.26	4.25	**0.018**

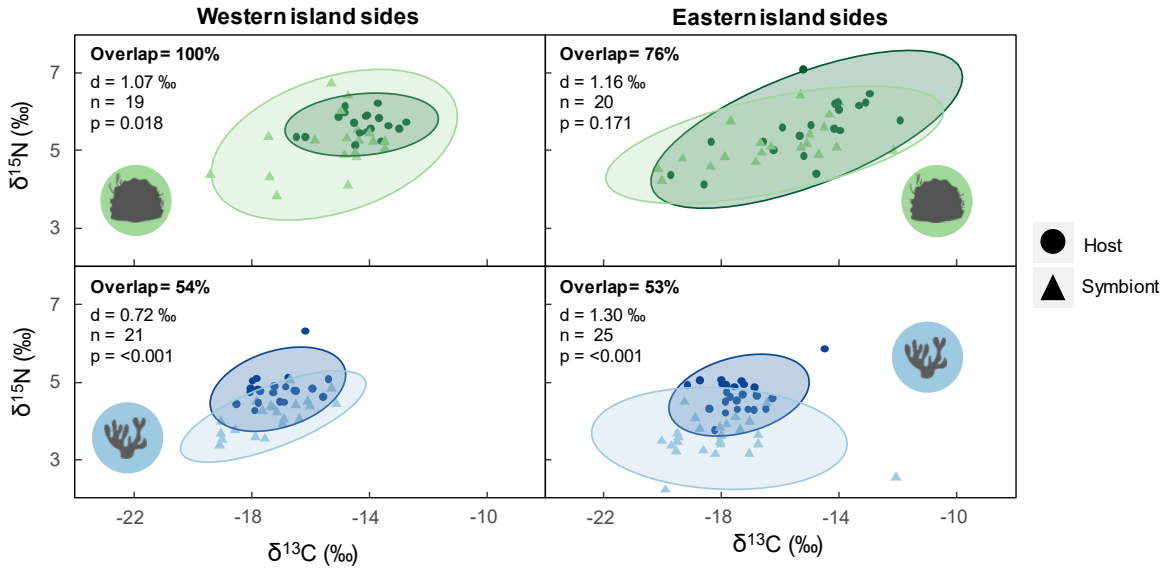

Figure 5: Isotopic biplots of coral host and symbiont at western LAIW exposed and eastern LAIW sheltered island sites. Porites host and symbiont in darker green and lighter green, respectively, and Pocillopora host and symbiont in darker blue and lighter blue, respectively. 95% SIBER standard ellipses corrected for sample size (SEAc) are fitted for both fractions and their overlap as a proportion of host ellipses is stated. P values from Hoteling T^2 test analyzing whether host and symbionts occupy distinct isotopic niches. d= Euclidean centroid distance, n=number of coral holobionts.

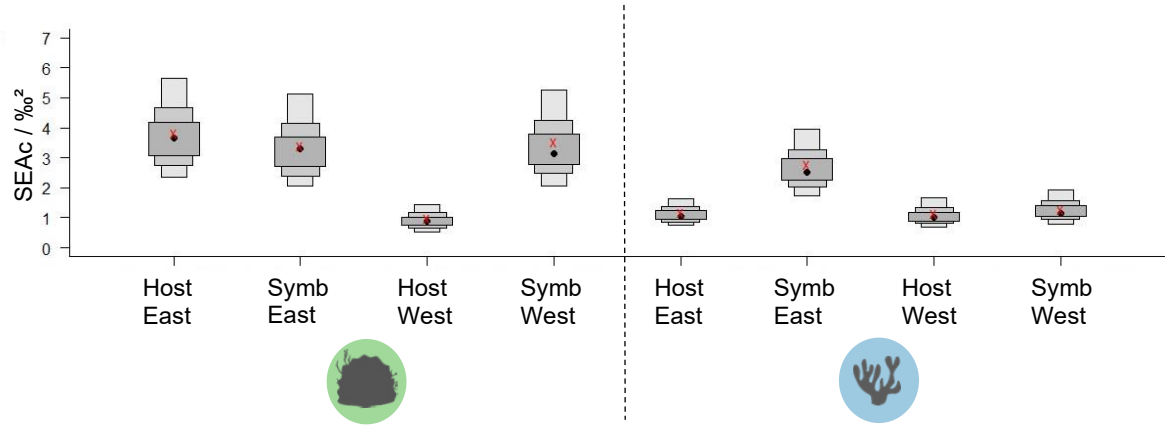

Figure 6: Size and certainty of Standard Ellipse Area corrected for sample size (SEAc) of Porites (left) and Pocillopora (right). Gradations denote 50%, 75% and 95% credibility intervals. Distributions were calculated via Bayesian inference in SIBER, which uses an Inverse Wishart prior on the covariance matrix and a normal prior on the means. Black dot shows the mode, while red cross shows the maximum likelihood ellipses. Symb=dinoflagellate endosymbiont.

Fatty acid analyses

A total of 51 FA and fatty alcohols were successfully identified in separated coral host and symbiont fractions using external standards (Supplement Table 1). Prior to deeper examination log ratio analysis (LRA) was performed for an initial inspection of FA profile variation across species, sites and host and symbiont fractions (Figure 7). Each species host fraction was distinct from their symbiont fraction indicating clear differences in coral host and symbiont FA profiles. Interestingly, both, the host and the symbiont fractions of *Pocillopora* diverged from *Porites* as well. However, samples from western and eastern sites only showed slight differences in location for *Porites* and completely overlapped in *Pocillopora*. This separation could also not be enhanced by conducting LRA on each species separate, nor by exclusively looking at a single species host fraction (Supplement Figure 2). In addition to LRA, total FA per surface area and putative FA health and trophic markers were calculated.

FA trophic markers suggest a slight increase in heterotrophic input in *Porites* from LAIW exposed reefs. Total lipids per surface area (Figure 8a) in *Porites* host fractions from LAIW exposed western reefs were significantly higher than in *Porites* host fractions from LAIW sheltered eastern reefs (GLM, p=0.001, Supplement Table 6). Although this effect can be seen for both islands, post hoc comparison did not find a significant difference of each islands eastern site compared to its western site (Supplement Table 7). *Porites* symbiont fraction show the same pattern although to a lesser and non-significant degree (GLM, p=0.054, Supplement Table 6). The autotrophy marker EPA : DHA was significantly lower in *Porites* from LAIW exposed western sites (Figure 8b; GLM, p=0.023, Supplement Table 6). The same pattern of trophic markers indicating more heterotrophy of *Porites* on LAIW exposed sites can be seen in the PUFA to SFA ratio (ANOVA, p=0.043, Supplement Table 6), and in the Animal derived FA to

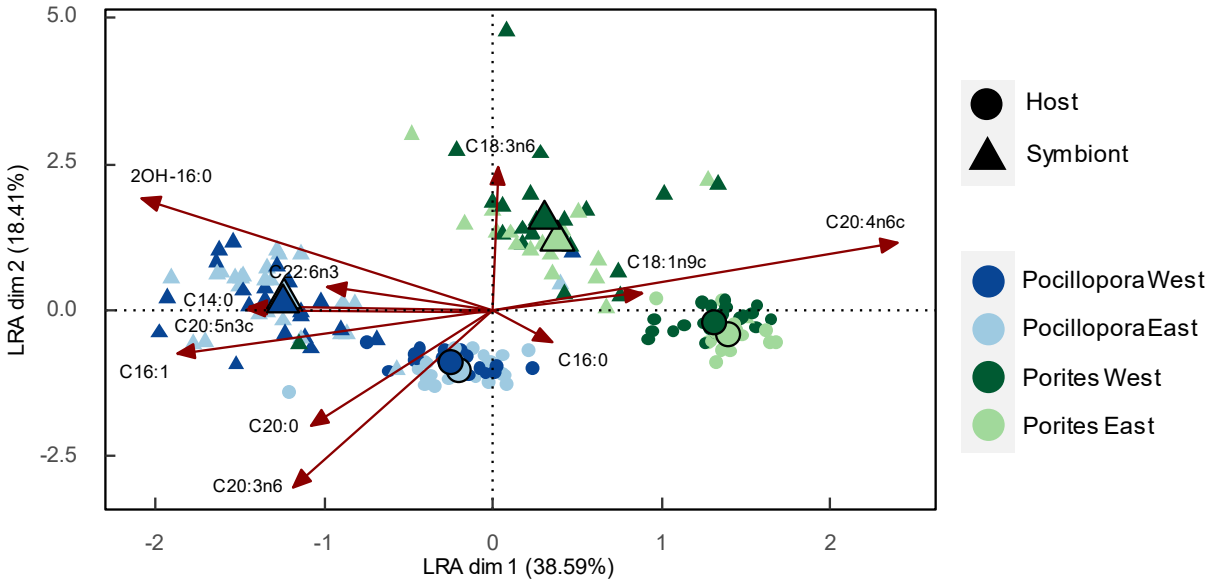

Figure 7:Log ratio analysis of all 51 fatty acid / fatty alcohols. Separated host (circle) and symbionts (triangle) of Porites (green) and Pocillopora (blue) from LAIW exposed western and LAIW sheltered eastern island sites of Racha and Miang. Centroids of each group are indicated by larger symbols with a black outline. Components that contribute highly to the seperation are shown with an arrow indicating direction and weight of the influence.

photosynthetically derived FA ratio (non-significant, ANOVA, p=0.051, Supplement Table 6). In contrast, neither LC-MUFA concentration nor C18:1n-9 : C18:1n-7 showed significant differences, although on Miang C18:1n-9 : C18:1n-7 was slightly higher in *Porites* host from the LAIW sheltered eastern reef (Figure 9). Interestingly, PUFA : SFA was much higher in *Porites* symbiont fractions from LAIW exposed sites (ANOVA, p=0.001, Supplement Table 6).

Pocillopora host fractions exhibited a different pattern in FA trophic markers. Although they demonstrated slightly higher lipids on LAIW exposed sites on both islands, this difference was not significant (GLM, p=0.378, Supplement Table 6). Symbiont fractions did show significantly higher FA per surface area on LAIW exposed sites (ANOVA, p=0.008, Supplement Table 6). Even so, the significant interaction effect of site and island (p=0.037) in addition to the results of post hoc pairwise comparison suggest that this is only true for Miang (EMM, p=0.008, Supplement Table 7) and not for Racha (EMM, p=0.969, Supplement Table 7).

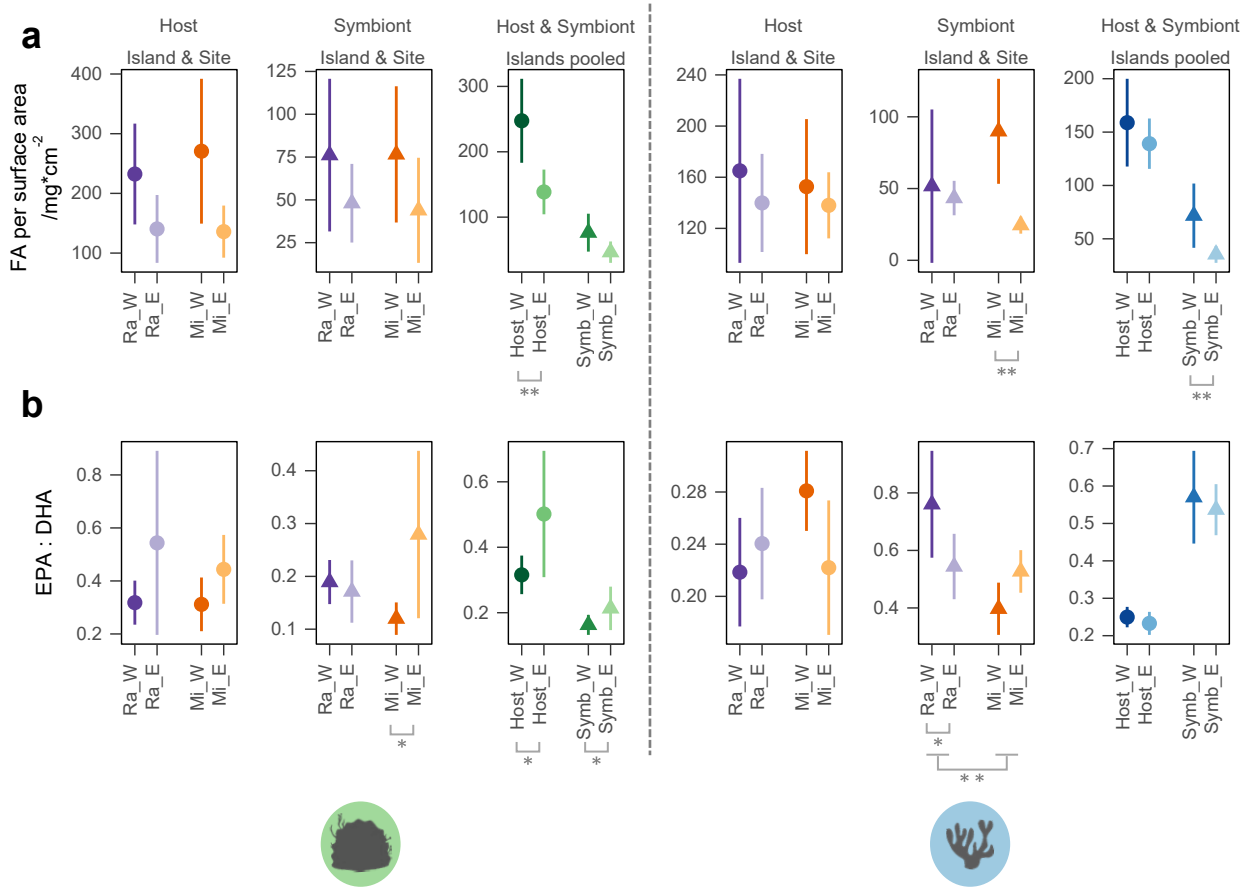

*Figure 8: Mean + 95% confidence interval of (a) total lipids per surface area and (b) the autotrophy marker EPA : DHA of separated coral host and symbiodinium fractions of Porites (left) and Pocillopora (right). Coral originated from LAIW exposed western sites (W) and LAIW sheltered eastern sites (E) of the islands Racha (Ra) and Miang (Mi) in the Andaman Sea. Significant differences assessed by two-factorial ANOVA or generalized linear models with post hoc estimated marginal means with Tukey HSD correction (p <0.001***, < 0.01**, <0.05*).*

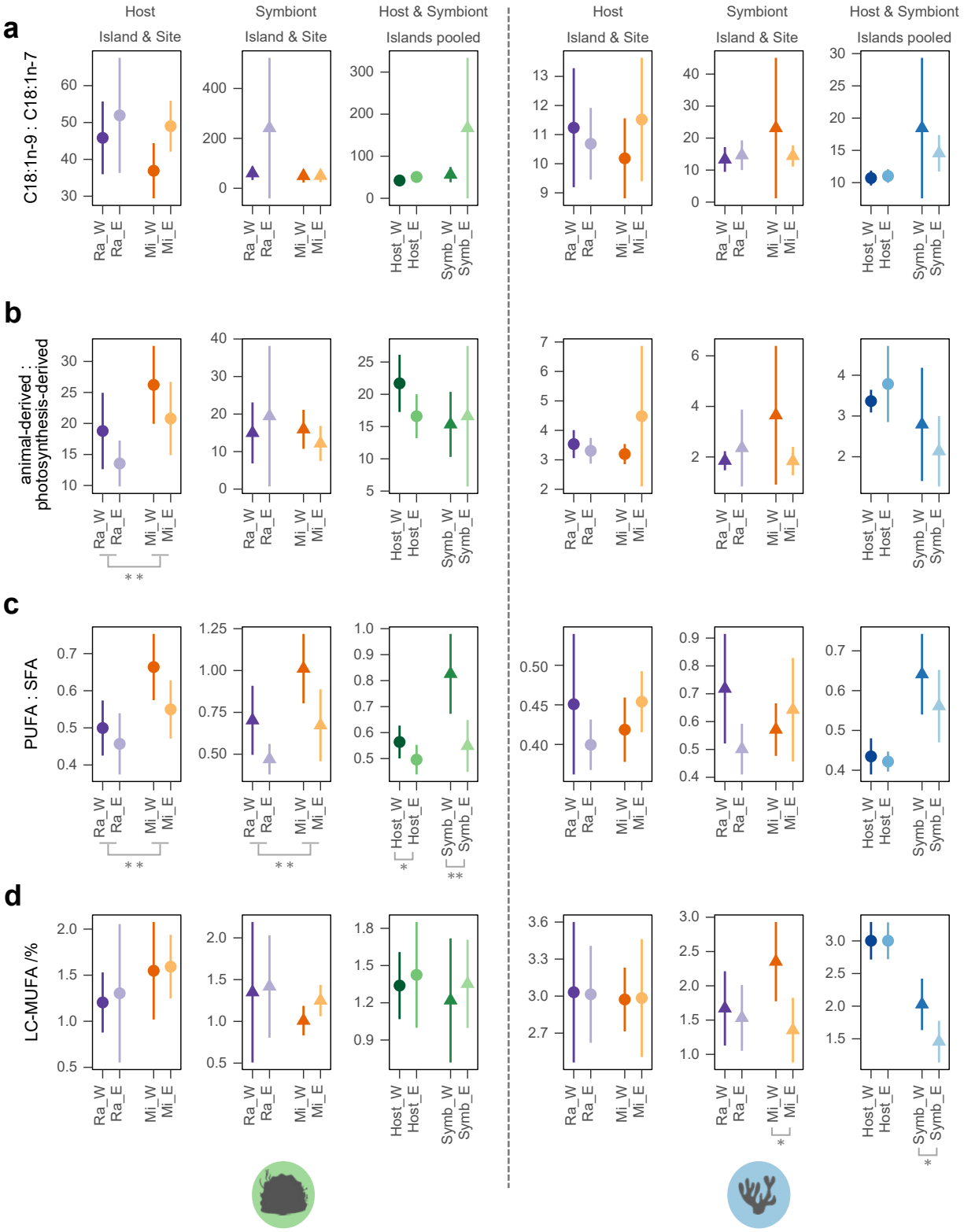

*Figure 9: Mean + 95% confidence interval of putative fatty acid trophic markers calculated for separated coral host and symbiodinium fractions of Porites (left) and Pocillopora (right). Coral originated from LAIW exposed western sites (W) and LAIW sheltered eastern sites (E) of the islands Racha (Ra) and Miang (Mi) in the Andaman Sea. (a) C18:1n-9 : C18:1n-7 (b) Animal-derived fatty acid : photosynthesis derived fatty acid (c) PUFA : SFA and (d) percent of long chain monounsaturated fatty acids. Significant differences assessed by two-factorial ANOVA or generalized linear models with post hoc estimated marginal means with Tukey HSD correction (p <0.001***, < 0.01**, <0.05*).*

LC-MUFA concentration were strikingly similar in *Pocillopora* hosts at all sites but were significantly elevated in the symbiont fractions from LAIW exposed sites compared to symbionts from LAIW sheltered sites (ANOVA, p=0.021, Supplement Table 6). This difference was facilitated mainly by the large difference on Miang which was also significant in pairwise comparison (EMM, p=0.028, Supplement Table 7). While the other trophic markers (PUFA : SFA, EPA : DHA, C18:1n-9 : C18:1n-7, Animal derived FA : photosynthesis derived FA) all indicated marginally higher heterotrophy on Rachas exposed site compared to its sheltered site, they had the opposite relationship with site on Miang. This suggests an interaction effect of the factors site and island for these markers, yet, the interaction term

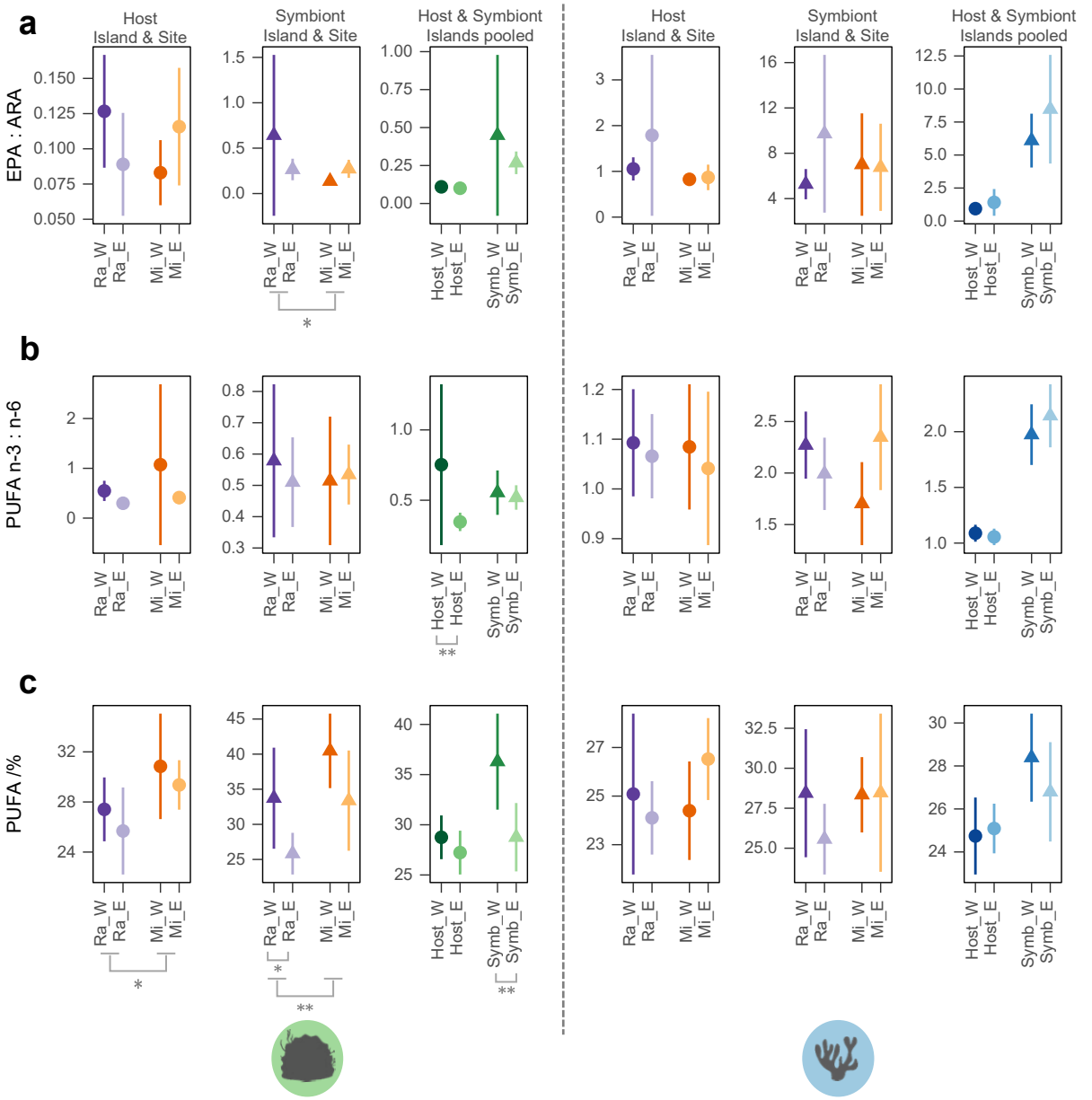

*Figure 10: Mean + 95% confidence interval of putative fatty acid health markers calculated for separated coral host and symbiodinium fractions of Porites (left) and Pocillopora (right). Coral originated from LAIW exposed western sites (W) and LAIW sheltered eastern sites (E) of the islands Racha (Ra) and Miang (Mi) in the Andaman Sea. (a) EPA : ARA, (b) PUFA n-3 : PUFA n-6, (c) PUFA as percent of all FA. Significant differences from generalized linear models and post hoc estimated marginal means with Tukey HSD correction (p <0.001***, < 0.01**, <0.05*).*

was only significant in the EPA : DHA ratio (Supplement Table 6, ANOVA, p=0.028). A heatmap with the effect sizes of all trophic markers was created to get an overview of all results (Figure 11).

Health markers showed differing patterns for *Porites* and *Pocillopora* (Figure 10). *Porites* host tissue from LAIW exposed western sites was characterized by a higher PUFA n-3 : n-6 ratio (GLM, p=0.003, Supplement Table 4) and a higher percent of PUFA (non-significant, ANOVA, p=0.275, Supplement Table 4). This was consistent throughout both islands although post hoc test did not show this to be significant after Tukey HSD correction for either ratio. EPA : ARA ratio deviated from this pattern and demonstrated an interaction effect of island and site (GLM, p=0.037, Supplement Table 4). Specifically, *Porites* host from Rachas LAIW exposed site had a higher ratio than those from Rachas eastern site while the inverse was true for Miang (neither one significant in post hoc test, Supplement Table 5). Notably, EPA : ARA was incredibly low in all *Porites* host samples, with mean values of all groups below 0.15, driven by the large amount of ARA (Supplement Figure 3). In total, FA health markers indicated a slightly healthier coral phenotype in *Porites* from LAIW exposed western sites. While these ratios cannot simply be interpreted as health markers in the symbiont fraction as they are for the host fraction, it should be noted that PUFA concentration was significantly higher in *Porites* symbionts from LAIW exposed sites (GLM, p=0.004, Supplement Table 4). Post hoc EMM showed a significant difference of Racha west to Racha east as well (EMM, p=0.049, Supplement Table 5).

In *Pocillopora* no significant differences between LAIW exposed and LAIW sheltered sites were found in any of the health markers for either host or symbiont fraction. In fact, the only significance found in any of the six models was the interaction of site and island for the ratio of n-3 to n-6 PUFAs in *Pocillopora* symbionts (ANOVA, p=0.017, Supplement Table 4). However, pairwise comparison did not reveal any single pair to be significantly different (Supplement Table 5). An overview of the effect sizes of all trophic markers in coral host fractions is given in Figure 11.

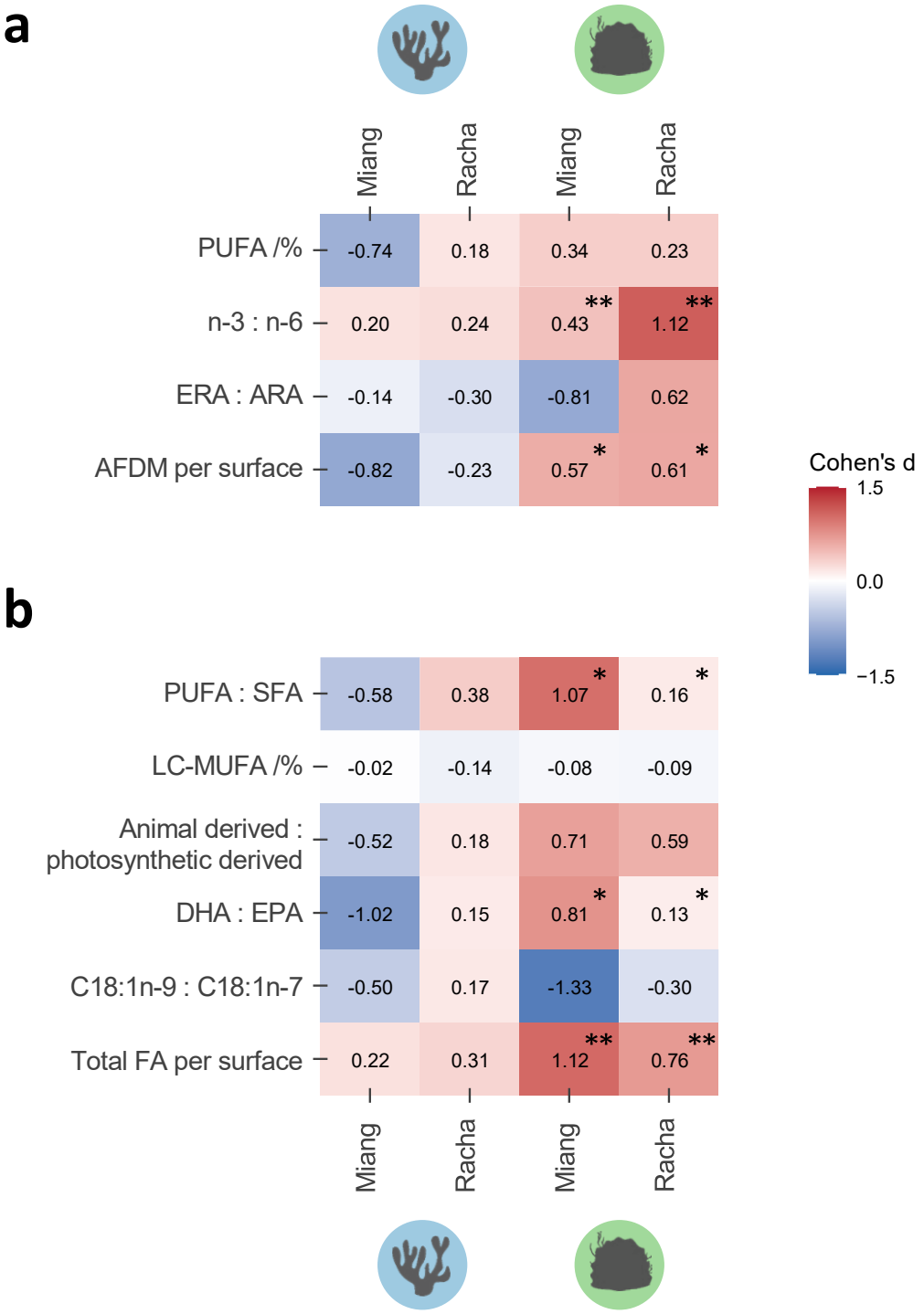

*Figure 11: Overview of (a) Health markers and (b) fatty acid trophic markers calculated for Pocillopora (left, blue) and Porites (right, green) host fractions of the islands Miang and Racha in the Andaman Sea. Values are Cohen's d effect size of LAIW exposed site - LAIW sheltered site. Note that the autotrophy marker EPA : DHA was flipped to DHA : EPA to allow for a consistent interpretation of values >0 = higher heterotrophy / better health status LAIW exposed sites. Significant differences of the overall site factor in models with DV~Island*site, not of pairwise comparison within islands! (p <0.001***, < 0.01**, <0.05*) No significant differences within islands in any pairwise comparison via estimated marginal means with Tukey HSD correction.*

Discussion

In this thesis I hypothesized that FA and SI trophic markers would show corals increased heterotrophy on LAIW exposed reefs, which could then explain their elevated thermal tolerance. This is not the case for *Pocillopora* who exhibits little variation in FA markers across sites with small tendencies of elevated heterotrophy on Rachas LAIW exposed site but also on Miangs sheltered site. Additionally, SIBER analysis of both islands pooled does not show any change from LAIW exposed sites to LAIW sheltered sites. Therefore, $H0_A$ (FA and SI heterotrophy markers will show no significant differences between corals from LAIW exposed and LAIW sheltered sites, indicating the same trophic strategy on a population level) cannot be rejected for *Pocillopora*. Similarly, putative health markers do not show a coherent picture and non-significant variation with small effect sizes. Thus, $H0_B$ (FA health markers and biomass per surface area will show no difference between corals from LAIW exposed and LAIW sheltered sites) cannot be rejected either. *Porites* does show slight differences in trophic markers, which are in parts significant. The effect sizes are small on Racha, but higher on Miang. However, SIBER analysis does not indicate higher heterotrophy on LAIW exposed sites. While there is a strong tendency towards increased heterotrophy on Miangs LAIW exposed site, there is arguably insufficient evidence against the $H0_A$ if Racha is considered as well. Health markers in *Porites* are higher on LAIW exposed sites with the only exception of EPA : ARA on Miang. Effect sizes of both islands are more similar than they were in the trophic markers and the differences in biomass per surface area and n-3 : n-6 were significant. There is more of an argument to be made about rejecting the $H0_B$ in *Porites* as they do show indication of an enhanced health status on LAIW exposed sites. Yet, from a strictly conservative standpoint it would have to be rejected as well, as EPA : ARA ratio and the non-significant difference in PUFA concentration give reasonable doubt. In regard to the research questions defined in this thesis the results demonstrate that neither $H0_A$ nor $H0_B$ can be rejected if *Porites*, *Pocillopora* and both islands are considered collectively. Consequently, shift in trophic strategy does not explain the superior heat resistance of LAIW exposed corals. In the following I will explain and contextualize these findings in more detail. Furthermore, I will highlight other insights that can be derived from the dataset.

Firstly, $\delta^{13}C_{H\text{-}S}$ being positive in virtually all corals in this thesis should be addressed. Commonly, $\delta^{13}C_{H\text{-}S}$ is interpreted as lowering with increases in heterotrophy. This concept mainly originates from a seminal paper by Muscatine et al. who measured $\delta^{13}C_{H\text{-}S}$ in corals at differing depths (Muscatine, Porter and Kaplan, 1989). While symbiont $\delta^{13}C$ declined with depth, host tissue $\delta^{13}C$ dropped faster, leading to $\delta^{13}C_{H\text{-}S}$ becoming lower with depth. The reduction of symbiont $\delta^{13}C$ was explained as a result of

decreased photosynthetic activity which allowed for increased discrimination against the heavy isotope ^{13}C. The larger depletion in host tissue $\delta^{13}C$ was explained as the coral incorporating higher amounts of zooplankton and POM which is depleted in $\delta^{13}C$ compared to the coral. The interpretation of lower $\delta^{13}C_{H\text{-}S}$ being indicative of higher heterotrophy makes sense when an autotrophic state is characterized by $\delta^{13}C_{H\text{-}S}$ being around zero. Divergence of host from symbiont $\delta^{13}C$ is then due to a decline in host $\delta^{13}C$ as food sources are more $\delta^{13}C$ depleted than shallow water corals e.g. zooplankton with typically ~-20‰ $\delta^{13}C$ (Muscatine, Porter and Kaplan, 1989; Roder *et al.*, 2010; Price *et al.*, 2021) and POM with similarly depleted $\delta^{13}C$ values (Ramaswamy *et al.*, 2008; Nahon *et al.*, 2013; Price *et al.*, 2021). This seems to be the general case and decline in $\delta^{13}C_{H\text{-}S}$ is often applied as a coral heterotrophy marker (Nahon *et al.*, 2013; Fox *et al.*, 2018; Williams *et al.*, 2018). However, in this thesis coral host were less $\delta^{13}C$ depleted (less negative) than their symbionts, creating positive $\delta^{13}C_{H\text{-}S}$ values. This is unusual but not unprecedented (Wall *et al.*, 2020; Price *et al.*, 2021; Chapron *et al.*, 2022). Price et al. used multiple SI approaches to compare trophic strategy of seven coral species (Price *et al.*, 2021). Four off the seven species had exclusively positive $\delta^{13}C_{H\text{-}S}$. Furthermore, they found that $\delta^{13}C_{H\text{-}S}$ seemed to be elevated in more heterotrophic species, challenging the widely accepted interpretation of this marker (at least when comparing different species). They did however not offer an explanation on how coral hosts can become 1-2‰ $\delta^{13}C$ enriched compared to their symbionts. Wall et al. analyzed $\delta^{13}C_{H\text{-}S}$ in mesophotic corals along a light gradient (Wall *et al.*, 2020). They found $\delta^{13}C_{H\text{-}S}$ becoming more positive with increased depth, which is opposite to the findings by Muscatine et al.. They hypothesize $\delta^{13}C_{H\text{-}S}$ becoming more positive is reflective of optimal symbiont densities with minimal cell shading resulting in maximized net photosynthesis but give little context how they came to this conclusion.

If the observed positive divergences in $\delta^{13}C$ of coral hosts from symbionts by ~1-2‰ in this study was due to feeding, the food source would have to be $\delta^{13}C$ enriched compared to the photosynthates supplied by the symbionts. In the Andaman Sea food source $\delta^{13}C$ seems to be similar to other regions, with values of –22.3 ± 0.11‰ measured in 2008 (Roder *et al.*, 2010) and POM at ~-20‰ $\delta^{13}C$ measured in the sediments in the northern Andaman Sea in 2003 (Ramaswamy *et al.*, 2008). Even though $\delta^{13}C$ are subject to spatiotemporal variations and zooplankton and (suspended) POM $\delta^{13}C$ could be quite different at the sampling location in 2018 it seems unlikely that they shifted to values above the here measured symbiont $\delta^{13}C$ (-18.50‰ - -14.18‰, Supplement Table 3). Therefore, feeding does not seem a likely explanation for the positive $\delta^{13}C_{H\text{-}S}$ found in this thesis and the reasoning behind coral host being relatively $\delta^{13}C$ enriched compared to their symbionts remains unknown. Isotropic fractionations in complex reciprocal carbon exchanges between both partners might offer an explanation and should be investigated. Understanding the underlying mechanisms marks an interesting field of study and could challenge the commonly accepted interpretations of $\delta^{13}C_{H\text{-}S}$.

Various insights were gained from LRA analysis. *Pocillopora* and *Porites* clearly occupied different positions, reflecting clear differences in FA profiles on a species level. This enforces the findings of other studies that FA profiles in corals are heavily species specific (Imbs *et al.*, 2010, 2014; Kim, Baker, *et al.*, 2021). Symbionts also occupied notably distinctive positions from their hosts, confirming successful tissue separation. Experimental evidence shows, that the same symbiont clade has differing FA profiles depending on coral host species, likely due to different FA being transferred from the host (Imbs *et al.*, 2014). However, there is very little research how much Symbiodinium FA profiles in symbioses with the same coral hosts are dependent on symbiont clade. As FAs are also transferred from the symbiont to the coral at high quantities, symbiont taxa specific FA profiles could have an impact on host FA profiles as well (Revel *et al.*, 2016). In the present dataset symbiont taxa has not been assessed. In the Andaman Sea *Porites lutea* seem to be dominated by the ITS-2 symbiont of the genotype C15 (Buerger *et al.*, 2015), therefore an impact of differing symbiont compositions on *Porites* FA profiles could be considered small. Unfortunately, there is no recent data for dinoflagellate composition of *Pocillopora verrucosa* for the Andaman Sea. The influence of symbiont taxa on symbiont FA profiles and host FA profiles can therefore not be assessed. While LRAs separated FA profiles on a species and symbiotic partner level, they failed to show clear separations of corals from LAIW exposed island sites and corals from LAIW sheltered island sites, suggesting similarities in full FA profiles.

Trophic strategy in *Pocillopora* seems to be quite similar on exposed and sheltered reefs with none of the six putative FA trophic markers being significantly different. Total FA per surface area was slightly higher on LAIW exposed sites and LC-MUFA did not show any difference. All other FA trophic markers followed the trend of indicating marginally higher heterotrophy on Rachas exposed site compared to its sheltered site but the opposite on Miang. In the univariate SI markers $\delta^{15}N_{H\text{-}S}$ was slightly higher on Miangs exposed site, indicating marginally higher heterotrophy contrasted by $\delta^{13}C_{H\text{-}S}$ which was also higher on Miangs exposed site commonly interpreted as a decrease in heterotrophy (Muscatine, Porter and Kaplan, 1989). Energy surplus in the coral holobiont through an increase in heterotrophy can in turn increase symbiont densities and thus photosynthesis (Houlbrèque *et al.*, 2004; Houlbrèque and Ferrier-Pagès, 2009). In the current study, biomass per surface area of the symbiont fractions was lower on LAIW exposed sites in all groups except for *Pocillopora* on Miang, providing evidence against a general shift towards more heterotrophy. Still, it should be considered how an increase of both, heterotrophy and autotrophy at the same time would be visible in the data. In such a scenario, the concurrent increase of heterotrophic and photosynthetic derived components could mask the effects of higher heterotrophy in FA trophic markers to some extent. However, if this was indeed the case, a difference in host SEAc overlap in SIBER analysis should be clearly visible signifying host and symbiont fraction utilizing different resource pools. This is not the case, as *Pocillopora* host SEAc overlap was the same for LAIW exposed and LAIW sheltered corals. Collectively, there is no indication of a shift in

trophic strategy for *Pocillopora* in response to LAIW. Thus, other factors seem to be responsible for the small changes observed in trophic markers.

Evaluating a possible change in trophic strategy due to LAIW exposure is more complex for *Porites*. FA trophic markers all show slightly higher heterotrophy on exposed sites and the differences observed in total lipids per surface area and in the ratios EPA : DHA and PUFA : SFA were statistically significant. Concentration of the herbivorous copepod marker LC-MUFA was low throughout all sampling groups of both, *Pocillopora* and *Porites*. *Pocillopora* from LAIW sheltered Racha site had the highest concentrations at 3.03 ± 0.9%, while corals that feed extensively on herbivores show concentrations of 5-6% (Veronica Z Radice *et al.*, 2019). This could lead to interpretations of herbivorous copepods playing a small role in the coral trophic systems of the Andaman Sea. However, it must be emphasized that only C20:1n9 and C22:1n9 could be identified in the FA profiles with the external standards used (SUPELCO® 37 component FAME mix; Bacterial Fatty Acid Methyl Esther mix (BAME)). The LC MUFA marker commonly includes the n-7 and n-11 fatty acids of C20 and C22 (Brett, Müller-Navarra and Persson, 2009; Veronica Z Radice *et al.*, 2019). In the context of this thesis dataset a consistently low concentration of LC MUFAs rather indicates a stable role of herbivorous copepods as food source throughout islands and sites. Other FA tropic markers in *Porites* show a tendency of an island effect in relation to LAIW exposure as they did in *Pocillopora*. However, where *Pocillopora* showed opposing effects of LAIW exposure on Miang and Racha, *Porites* FA trophic markers show a consistent trend but with notably larger effect sizes on Miang. The univariate SI trophic markers $\delta^{13}C_{H\text{-}S}$ and $\delta^{15}N_{H\text{-}S}$ did also not differ by a lot between sites of each island. Only $\delta^{13}C_{H\text{-}S}$ was noticeably lower on Miangs LAIW exposed site, indicating higher heterotrophy (sensu Muscatine). Interpretation of trophic strategy in response to *Porites* gets more complicated when results of SIBER analysis are considered as well. Here *Porites* host SEAc showed a 100% overlap. Importantly, this complete overlap is not meant to suggest a complete absence of heterotrophy. Indeed, when the 40% SEA_C overlap is considered (Supplement Figure 1) it is apparent that the data does not imply full resource sharing between host and symbiont on LAIW exposed sites. Still, larger overlap on exposed sites indicates higher reliance on autotrophy which conflicts with the results of FA analysis. While data of both islands was pooled for SIBER analysis it is unlikely that this is the reason for the contradictory result. In SIBER analysis data from different locations is regularly pooled, as the required sample size can often not be obtained on smaller spatial scales (Conti-Jerpe *et al.*, 2020; Thibault *et al.*, 2022). In fact, one major advantage of using SIBER is the removal of spatiotemporal variations in isotope baselines, as paired coral host and symbionts inherently share sampling time and space. Naturally, the results of pooled locations are ellipses that essentially average the ecological variation of all locations, i.e. the *Pocillopora* ellipses in this thesis. Yet, pooling locations should not result in an overestimation of ellipses overlap (Conti-Jerpe *et al.*, 2021). Isotopic niche of the Porites host fraction from LAIW exposed sites was much smaller than all

other *Porites* host and symbiont niches and is likely the main reason for the complete overlap. It also explains why Hotelling t-test indicated significantly different isotopic niches even though host fraction was completely overlapped by the symbiont fraction. While a smaller SEAc could imply a much narrower trophic niche for Porites host from LAIW exposed sites, it is more likely an artifact resulting from the small sample size. For one, ecological variance that broadens isotopic niche might have been missed but more importantly the correction for sample size in SEAc is most accurate in sample sizes above 30 (Syväranta *et al.*, 2013). While the other sampling groups also had smaller sample counts, LAIW exposed *Porites* had the lowest. Stable isotope analysis in itself has some limitations in corals and differing approaches can lead to different results (Price *et al.*, 2021). Moreover, the allocation of autotrophic or heterotrophic SI sources to host and symbiont tissues can vary with prior thermal and nutritional exposure (Baumann *et al.*, 2014; Krueger *et al.*, 2018). Differences in the ratio of carbon : lipid : protein also influence bulk $\delta^{13}C$ signature in coral hosts (Wall *et al.*, 2019) and could have been an issue here as western *Porites* had significantly higher lipid concentrations. Additionally, symbiont type can influence stable isotope values of the coral host unrelated to their energy acquisition (Wall *et al.*, 2020). Nonetheless, even with these limitations in mind a major shift towards more heterotrophy on LAIW exposed sites should be visible to some degree and certainly not result in a higher SEAc overlap compared to LAIW sheltered sites.

In conclusion, the data does not confirm a collective trophic shift of corals in response to LAIW. FA trophic markers in *Porites* show slight increases in heterotrophy on Miang and a smaller increase on Racha. SIBER analysis of both islands pooled does not support more heterotrophy on LAIW exposed sites. *Pocillopora* shows even less indication of a shift towards more heterotrophy due to LAIW exposure, with marginal differences in trophic markers throughout all groups and the direction of effect differing on Miang and Racha. Wall et al. found elevated bleaching resistance in LAIW exposed *Porites* and *Pocillopora* compared to conspecifics from LAIW sheltered sites (Wall, Doering, *et al.*, 2023). The corals used in their study were sampled together with the Racha corals analyzed in this thesis. The lack of increased heterotrophy for *Pocillopora* and only negligible increases in heterotrophy for *Porites* from Racha strongly suggests that the amplified bleaching resistance of LAIW exposed corals cannot be attributed to a change in trophic strategy.

On first glance, no shift towards more heterotrophy in LAIW exposed corals contrasts the findings of Roder et al., 2010. They discovered that *Pocillopora meandrina* from LAIW exposed sites in the Andaman Sea show the ability to feed more than those from LAIW sheltered sites under light exclusion. $\delta^{13}C$ decreased significantly more in LAIW exposed corals than in sheltered corals. Yet importantly, at control light conditions $\delta^{13}C$ values were equal. It allows for the interpretation that LAIW exposed corals do possess the ability to rapidly increase heterotrophic feeding if energy requirements demand it and food is available but maintain similar trophic strategy under normal conditions. The ability of corals

from LAIW exposed sites to increase feeding quicker than their conspecifics from LAIW sheltered sites might be due to them being used to an environment characterized by reoccurring sudden changes.

The results of no collective shift in trophic strategy on LAIW exposed sites further seem to be at odds with recent findings by Fox *et al.*, 2023. They found that El Niño heatwaves increased cold water pulses through internal waves on the Palmyra atoll. During these periods of increased internal wave action *Pocillopora meandrina* demonstrated increased heterotrophy, implying higher food acquisition through internal wave supplied nutrients. El Niño heatwaves are among the most stressful events corals can experience. Fox et al. state that even though internal waves mitigated some heat stress by introducing cold water pulses temperatures were still elevated. Following, the interpretation from above it could be possible that *P. meandrina* increased feeding effort, not in response to internal waves providing food sources alone, but only in addition with the high energy demand associated with heat stress.

The question remains as to why corals should only show limited ability to utilize the enhanced flux of particulate organic matter (POM) and zooplankton mass provided by LAIW, which was found by Roder *et al.,* 2010. Deep water pulses through LAIW are characteristically short and intense (Schmidt *et al.*, 2012; Reid *et al.*, 2019). Increased plankton and particulate organic matter in LAIW exposed sites is possibly only present during these cold-water pulses and quickly washes over the reef. In fact, plankton and POM concentrations were found to be similar on LAIW exposed and sheltered sites by Roder et al. Only the combination with the higher mean daily current speeds on LAIW sites led to an interpretation of increased daily plankton and POC fluxes. Corals might show limited ability to quickly increase feeding when deep water pulses carrying zooplankton and POM wash over them. Pacherres, Schmidt and Richter, 2013 found that simulated LAIW (cold water pulses with lower pH) led to polyp retraction in *Porites lutea*. Furthermore, under simulated LAIW food presence did no longer result in polyp extension observed in stable conditions. Even though corals with LAIW history showed acclimatization and only retracted their polyps slightly compared to corals unfamiliar with LAIW, minor retractions in the first minutes after LAIW arrival in addition to changes in POM/zooplankton concentrations being only short lived might explain why corals are not able to utilize the provided food sources to their full extent.

In addition to trophic markers, health markers were assessed in this thesis. *Pocillopora* host and symbiont fractions had slightly lower biomass on LAIW exposed sites. Overall, FA health markers were similar in *Pocillopora* from LAIW exposed and sheltered sites with none of the differences being significant. Health markers were also not in full agreeance with some markers indicating better health status in LAIW exposed corals and others the opposite. It can therefore be concluded that health status of *Pocillopora*, as assessed by FA markers, does not differ in response to LAIW exposure. Health markers in *Porites* were more aligned with each other and showed larger differences. LAIW exposed *Porites* significantly higher biomass in addition to differences in FA markers indicated them to be healthier.

Percent PUFA and n-3 to n-6 ratio were slightly elevated in LAIW exposed corals. PUFA was significantly higher not in the host but in the symbiont fraction signaling higher PUFA concentrations in the holobiont on LAIW exposed sites. EPA : ARA on Miang was the only marker deviating from the others suggesting enhanced health for sheltered *Porites.* EPA : ARA was also low throughout all *Porites* samples with mean ratios being tenfold lower than in *Pocillopora*. Furthermore, the lower EPA : ARA ratio in *Porites* from Miangs exposed site but also higher n-3 : n-6 PUFA ratio might indicate *Porites* maintains lower EPA : ARA levels but is able to readily synthesize EPA if anti-inflammation is required. Consequently, EPA : ARA might not be a reliable health marker in *Porites lutea*. Additionally, EPA : ARA ratio being much higher in *Pocillopora* should not be interpreted as them being healthier, but rather as species specific differences that were also evident in LRA.

Trophic strategy not explaining the superior bleaching resistance of LAIW exposed corals begs the question of which other processes could be responsible. LAIW exposed corals show lower calcification rates, lower coral heights and less reef development (Schmidt *et al.*, 2012; Wall *et al.*, 2012; Schmidt and Richter, 2013). Additionally, Roder et al. found an overall higher nutritional status including higher protein concentrations and higher biomass per surface area (Roder *et al.*, 2010, 2011). It could be possible that these findings are signs of a trade-off where LAIW exposed corals expend less energy for growth and rather store more energy which is known to reduce coral bleaching susceptibility (Anthony *et al.*, 2009; Tagliafico *et al.*, 2017). While total FA per surface area was characterized as a trophic marker in this thesis, it might rather be further indication for this trade-off. In *Porites* higher energy status on LAIW exposed sites is evident with significantly higher FA per surface area in addition to significantly higher biomass. Enhanced health status and higher energy reserves of LAIW exposed *Porites* contrasts with their lower coverage on western island sites (Brown, 2007; Schmidt *et al.*, 2012). This further corroborates a trade-off, where higher stress resistance and energy reserves result in less growth. LAIW exposed *Pocillopora* had slightly lower biomass per surface area, contrasting Roder et al.'s findings. However, they did show slightly increased total FA concentrations.

Exposed corals could also be acclimatized and stress hardened due to the periodic environmental variability via LAIW (Wall, Doering, *et al.*, 2023). Similarly enhanced bleaching resistance has been found in other coral populations subject to high frequent temperature fluctuations (Oliver and Palumbi, 2011; Safaie *et al.*, 2018). Some of this stress-hardening could possibly be attributed to transcriptional "frontloading" (Barshis *et al.*, 2013). Barshis et al. investigated gene expression of heat tolerant corals in tide pools, another highly variable habitat. Prior work had shown that corals from tide pools with higher variances had elevated heat stress resistance compared to corals from low to mid variance sites. Barshis et al. discovered that the corals from high variable tide pools had upregulated several stress genes under ambient conditions including genes for several heat shock proteins (e.g. Hsp70). Consequently, this frontloading enables these corals to react to stress quicker and with less rigorous

changes in their metabolism. It could be possible that corals from western island sites similarly frontload stress genes due to the periodic disturbances through LAIW, thereby enhancing their thermal tolerance. Frontloading could also explain the elevated Protein concentration observed in LAIW exposed corals.

Finally, a difference in microbiome of LAIW exposed and sheltered corals might offer an explanation for the differential in bleaching resistance. Doering et al. conducted microbiome transplantations from *Porites sp*. and *Pocillopora sp*. in high variance environments to conspecifics in low variance environments in the Andaman Sea (Doering *et al.*, 2021). For *Pocillopora sp.* this high variance site was the LAIW exposed site of Racha, where parts of the corals analyzed in this thesis originated from as well. Corals from the low variance sites demonstrated enhanced bleaching resistance after being inoculated with microbiome from the high variance sites. The study highlights the effects of the microbiome on heat resistance and shows that there are processes that allow corals in high variance sites to harbor beneficial microbiomes. For *Pocillopora* this was directly shown for the LAIW exposed site of Racha, and we can infer that it is probably similar to *Porites* at Racha and to other LAIW exposed sites in general.

The findings of this thesis together with the studies highlighted demonstrate, that microbiome, stress hardening and a trade-off are more likely explanations of the mechanisms behind the elevated bleaching resistance of LAIW exposed corals than shift in trophic strategy.

Conclusion

Heterotrophy and health markers in relation to LAIW exposure were not fully aligned and reveal a complex picture. Changes in coral trophic strategy in response to LAIW are demonstrated to be very nuanced in addition to being island and species dependent.

Siber analysis did not show any shift towards more heterotrophy on LAIW exposed sites for Pocillopora and even an increase in autotrophy for *Porites*. Conversely, FA trophic markers indicated slight increases in heterotrophy for LAIW exposed *Porites* with a larger effect on Miang compared to Racha. *Pocillopora* trophic strategy, as assessed by FA trophic markers, had a tendency towards island dependence and was very similar on all sites. Similar patterns were observed in FA health markers. *Pocillopora* shows little indication of an increased health status on LAIW exposed sites while *Porites* health status seems slightly enhanced.

The sample size in this thesis was not large enough for island specific SIBER analysis. More so, even the pooled data from both islands was below the recommended count. Additionally, some FA in putative trophic markers could not be identified with the FA analytics approach utilized here and possibly introduced some uncertainties in the results. Nevertheless, a collective shift in trophic strategy that is large enough to explain enhanced bleaching resistance of *Porites* and *Pocillopora* on LAIW exposed sites should be clearly visible in FA trophic markers and stable isotope markers throughout both islands and species with the dataset at hand. This is not the case. At this time, it seems more reasonable that other mechanisms are the driving factors behind the increased bleaching resistance observed in LAIW exposed corals. These include differences in energy allocation and microbiomes, in addition to stress hardening and transcriptional frontloading due to periodic disturbances via LAIW.

Future studies should verify the findings of this thesis by increasing the sample size to allow for separate SIBER analysis per island. Compound specific stable isotope analysis might further remove noise from the trophic SI signature introduced by differing relative amounts of lipids, proteins, and carbohydrates. Additionally, adopting a more targeted FA analysis approach that allows for the identification of all FAs involved in putative trophic markers could provide higher resolution on trophic strategy.

References

Al-Sarraj, R. and Forkman, J. (2023) 'Notes on correctness of p-values when analyzing experiments using SAS and R', *PLOS ONE*, 18(11), pp. 1–17. doi: 10.1371/journal.pone.0295066.

Anthony, K. R. N. *et al.* (2009) 'Energetics approach to predicting mortality risk from environmental stress: A case study of coral bleaching', *Functional Ecology*, 23(3), pp. 539–550. doi: 10.1111/j.1365-2435.2008.01531.x.

Bachok, Z., Mfilinge, P. and Tsuchiya, M. (2006) 'Characterization of fatty acid composition in healthy and bleached corals from Okinawa, Japan', *Coral Reefs*, 25(4), pp. 545–554. doi: 10.1007/s00338-006-0130-9.

Barshis, D. J. *et al.* (2013) 'Genomic basis for coral resilience to climate change', *Proceedings of the National Academy of Sciences of the United States of America*, 110(4), pp. 1387–1392. doi: 10.1073/pnas.1210224110.

Baumann, J. *et al.* (2014) 'Journal of Experimental Marine Biology and Ecology Photoautotrophic and heterotrophic carbon in bleached and non-bleached coral lipid acquisition and storage', *Journal of Experimental Marine Biology and Ecology*, 461, pp. 469–478. doi: 10.1016/j.jembe.2014.09.017.

Bindoff, N. L. *et al.* (2019) *Changing Ocean, Marine Ecosystems, and Dependent Communities*, *IPCC Special Report on the Ocean and Cryosphere in a Changing Climate*. doi: https://www.ipcc.ch/report/srocc/.

Bligh, E. G. and Dyer, W. J. (1959) 'A RAPID METHOD OF TOTAL LIPID EXTRACTION AND PURIFICATION', *Canadian Journal of Biochemistry and Physiology*, 37(8), pp. 911–917. doi: 10.1139/o59-099.

Bottino, N. R. *et al.* (1980) 'Seasonal and nutritional effects on the fatty acids of three species of shrimp, Penaeus setiferus, P. aztecus and P. duorarum', *Aquaculture*, 19(2), pp. 139–148.

Brett, M. T., Müller-Navarra, D. C. and Persson, J. (2009) 'Crustacean zooplankton fatty acid composition', in Kainz, M., Brett, M. T., and Arts, M. T. (eds) *Lipids in Aquatic Ecosystems*. New York, NY: Springer New York, pp. 115–146. doi: 10.1007/978-0-387-89366-2_6.

Brown, B. E. (2007) 'Coral reefs of the Andaman Sea - an integrated perspective', in Gibson R.N., Atkinson R.J.A., G. J. D. M. (ed.) *Oceanography and Marine Biology: an Annual Review*, pp. 173–194.

Buerger, P. *et al.* (2015) 'Temperature tolerance of the coral Porites lutea exposed to simulated large amplitude internal waves (LAIW)', *Journal of Experimental Marine Biology and Ecology*, 471, pp. 232–

239. doi: 10.1016/j.jembe.2015.06.014.

Chapron, L. *et al.* (2022) 'Natural Variability in Caribbean Coral Physiology and Implications for Coral Bleaching Resilience', *Frontiers in Marine Science*, 8(January), pp. 1–15. doi: 10.3389/fmars.2021.811055.

Conti-Jerpe, I. E. *et al.* (2020) 'Trophic strategy and bleaching resistance in reef-building corals', *Science advances*, 6(15), p. eaaz5443.

Conti-Jerpe, I. E. *et al.* (2021) 'Response to Comment on Trophic strategy and bleaching resistance in reef-building corals', *Science Advances*, 7(23), pp. 2–4. doi: 10.1126/sciadv.abd9453.

Costanza, R. *et al.* (2014) 'Changes in the global value of ecosystem services', *Global Environmental Change*, 26(1), pp. 152–158. doi: 10.1016/j.gloenvcha.2014.04.002.

Couturier, L. I. E. *et al.* (2020) 'State of art and best practices for fatty acid analysis in aquatic sciences', *ICES Journal of Marine Science*. doi: 10.1093/icesjms/fsaa121.

Dalsgaard, J. *et al.* (2003) 'Fatty acid trophic markers in pelagic marine environment', 4.

DeNiro, M. J. and Epstein, S. (1978) 'Influence of diet on the distribution of carbon isotopes in animals', *Geochimica et Cosmochimica Acta*, 42(5), pp. 495–506. doi: https://doi.org/10.1016/0016-7037(78)90199-0.

Doering, T. *et al.* (2021) 'Towards enhancing coral heat tolerance: a "microbiome transplantation" treatment using inoculations of homogenized coral tissues', *Microbiome*, 9(1), pp. 1–16. doi: 10.1186/s40168-021-01053-6.

Eakin, C. M., Sweatman, H. P. A. and Brainard, R. E. (2019) 'The 2014–2017 global-scale coral bleaching event: insights and impacts', *Coral Reefs*, 38(4), pp. 539–545. doi: 10.1007/s00338-019-01844-2.

Ferrier-Pagès, C. *et al.* (2010) 'Experimental assessment of the feeding effort of three scleractinian coral species during a thermal stress: Effect on the rates of photosynthesis', *Journal of Experimental Marine Biology and Ecology*, 390(2), pp. 118–124. doi: 10.1016/j.jembe.2010.05.007.

Figueiredo, J. *et al.* (2012) 'Ontogenetic change in the lipid and fatty acid composition of scleractinian coral larvae', *Coral Reefs*, 31(2), pp. 613–619. doi: 10.1007/s00338-012-0874-3.

Fisher, R. *et al.* (2015) 'Species richness on coral reefs and the pursuit of convergent global estimates', *Current Biology*, 25(4), pp. 500–505. doi: 10.1016/j.cub.2014.12.022.

Folch, J. *et al.* (1957) 'A simple method for the isolation and purification of total lipids from animal tissues', *J biol Chem*, 226(1), pp. 497–509.

Fox, J. and Weisberg, S. (2019) *An {R} Companion to Applied Regression*. Third. Thousand Oaks {CA}: Sage. Available at: https://socialsciences.mcmaster.ca/jfox/Books/Companion/.

Fox, M. D. *et al.* (2018) 'Gradients in Primary Production Predict Trophic Strategies of Mixotrophic Corals across Spatial Article', *Current Biology*, 28(21), pp. 3355-3363.e4. doi: 10.1016/j.cub.2018.08.057.

Fox, M. D. *et al.* (2019) 'Trophic plasticity in a common reef - building coral : Insights from δ 13 C analysis of essential amino acids', (August), pp. 2203–2214. doi: 10.1111/1365-2435.13441.

Fox, M. D. *et al.* (2023) 'Ocean currents magnify upwelling and deliver nutritional subsidies to reef-building corals during El Niño heatwaves', *Science Advances*, 5032. doi: 10.1126/sciadv.add5032.

Fry, B. and Sherr, E. B. (1989) '$δ$13C Measurements as Indicators of Carbon Flow in Marine and Freshwater Ecosystems', in Rundel, P. W., Ehleringer, J. R., and Nagy, K. A. (eds) *Stable Isotopes in Ecological Research*. New York, NY: Springer New York, pp. 196–229.

Fu, K. H. *et al.* (2012) 'Shoaling of large-amplitude nonlinear internal waves at Dongsha Atoll in the northern South China Sea', *Continental Shelf Research*, 37, pp. 1–7. doi: 10.1016/j.csr.2012.01.010.

Gibson, R. N., Atkinson, R. J. A. and Gordon, J. D. M. (2007) 'Coral reefs of the Andaman Sea—an integrated perspective', *Oceanography and marine biology: an annual review*, 45, pp. 173–194.

Graeve, M. and Greenacre, M. J. (2020) 'The selection and analysis of fatty acid ratios: A new approach for the univariate and multivariate analysis of fatty acid trophic markers in marine pelagic organisms', *Limnology and Oceanography: Methods*, 18(5), pp. 196–210. doi: 10.1002/lom3.10360.

Graeve, M., Kattner, G. and Hagen, W. (1994) 'Diet-induced changes in the fatty acid composition of Arctic herbivorous copepods: Experimental evidence of trophic markers', *Journal of Experimental Marine Biology and Ecology*, 182(1), pp. 97–110. doi: https://doi.org/10.1016/0022-0981(94)90213-5.

Graeve, M., Kattner, G. and Piepenburg, D. (1997) 'Lipids in arctic benthos: Does the fatty acid and alcohol composition reflect feeding and trophic interactions?', *Polar Biology*, 18(1), pp. 53–61. doi: 10.1007/s003000050158.

Greenacre, M. (2018) *Compositional Data Analysis in Practice*. Chapman & Hall / CRC Press.

Grottoli, A. G., Rodrigues, L. J. and Palardy, J. E. (2006) 'Heterotrophic plasticity and resilience in bleached corals', *Nature*, 440(7088), pp. 1186–1189. doi: 10.1038/nature04565.

Hansen, T., Burmeister, A. and Sommer, U. (2009) 'Simultaneous δ15 N, δ13 C and δ34S measurements of lowbiomass samples using a technically advanced high sensitivity elemental analyzer connected to an isotope ratio mass spectrometer', *Rapid Communications in Mass Spectrometry*, 23(21), pp. 3387–

3393. doi: 10.1002/rcm.4267.

Hartig, F. (2022) 'DHARMa: Residual Diagnostics for Hierarchical (Multi-Level / Mixed) Regression Models'. Available at: https://cran.r-project.org/package=DHARMa.

Hoegh-Guldberg, O., Pendleton, L. and Kaup, A. (2019) 'People and the changing nature of coral reefs', *Regional Studies in Marine Science*. Elsevier B.V., p. 100699. doi: 10.1016/j.rsma.2019.100699.

Houlbrèque, F. *et al.* (2004) 'Interactions between zooplankton feeding, photosynthesis and skeletal growth in the scleractinian coral Stylophora pistillata', *Journal of Experimental Biology*, 207(9), pp. 1461–1469. doi: 10.1242/jeb.00911.

Houlbrèque, F. and Ferrier-Pagès, C. (2009) 'Heterotrophy in tropical scleractinian corals', *Biological Reviews*, 84(1), pp. 1–17. doi: 10.1111/j.1469-185X.2008.00058.x.

Huffmyer, A. S. *et al.* (2021) 'Feeding and thermal conditioning enhance coral temperature tolerance in juvenile Pocillopora acuta'.

Hughes, A. D. and Grottoli, A. G. (2013) 'Heterotrophic compensation: A possible mechanism for resilience of coral reefs to global warming or a sign of prolonged stress?', *PLoS ONE*, 8(11), pp. 1–10. doi: 10.1371/journal.pone.0081172.

Hughes, T. P. *et al.* (2018) 'Spatial and temporal patterns of mass bleaching of corals in the Anthropocene', *Science*, 359(6371), pp. 80–83. doi: 10.1126/science.aan8048.

Imbs, A. *et al.* (2010) 'Distribution of lipids and fatty acids in corals by their taxonomic position and presence of zooxanthellae', *Marine Ecology Progress Series*, 409, pp. 65–75. doi: 10.3354/meps08622.

Imbs, A. B. *et al.* (2014) 'Diversity of fatty acid composition of symbiotic dinoflagellates in corals: Evidence for the transfer of host PUFAs to the symbionts', *Phytochemistry*, 101, pp. 76–82. doi: 10.1016/j.phytochem.2014.02.012.

Jackson, A. and Parnell, A. (2023) 'SIBER: Stable Isotope Bayesian Ellipses in R'. Available at: https://cran.r-project.org/package=SIBER.

Jain, T. *et al.* (2023) 'Differing Responses of Three Scleractinian Corals from Phuket Coast in the Andaman Sea to Experimental Warming and Hypoxia'.

Kabeya, N. *et al.* (2018) 'Genes for de novo biosynthesis of omega-3 polyunsaturated fatty acids are widespread in animals', *Science Advances*, 4(5), pp. 1–8. doi: 10.1126/sciadv.aar6849.

Kim, T., Baker, D. M., *et al.* (2021) 'Fatty acid profiles of separated host–symbiont fractions from five symbiotic corals: applications of chemotaxonomic and trophic biomarkers', *Marine Biology*, 168(11),

pp. 1–13. doi: 10.1007/s00227-021-03979-9.

Kim, T., Lee, J. C. Y., *et al.* (2021) 'Modification of fatty acid profile and biosynthetic pathway in symbiotic corals under eutrophication', *Science of the Total Environment*, 771. doi: 10.1016/j.scitotenv.2021.145336.

Kleypas, J. *et al.* (2021) 'Designing a blueprint for coral reef survival', *Biological Conservation*, 257, p. 109107. doi: 10.1016/j.biocon.2021.109107.

Krueger, T. *et al.* (2018) 'Temperature and feeding induce tissue level changes in autotrophic and heterotrophic nutrient allocation in the coral symbiosis – A NanoSIMS study', (August), pp. 1–15. doi: 10.1038/s41598-018-31094-1.

Legezynska, J., Kedra, M. and Walkusz, W. (2012) 'When season does not matter : summer and winter trophic ecology of Arctic amphipods', pp. 189–214. doi: 10.1007/s10750-011-0982-z.

Leichter, J. J. *et al.* (1996) 'Pulsed delivery of subthermocline water to Conch Reef (Florida Keys) by internal tidal bores', *Limnology and Oceanography*, 41(7), pp. 1490–1501. doi: 10.4319/lo.1996.41.7.1490.

Leichter, J. J., Helmuth, B. and Fischer, A. M. (2006) 'Variation beneath the surface: Quantifying complex thermal environments on coral reefs in the Caribbean, Bahamas and Florida', *Journal of Marine Research*, 64(4), pp. 563–588. doi: 10.1357/002224006778715711.

Lenth, R. V (2022) 'emmeans: Estimated Marginal Means, aka Least-Squares Means'. Available at: https://cran.r-project.org/package=emmeans.

Minagawa, M. and Wada, E. (1984) 'Stepwise enrichment of 15N along food chains: Further evidence and the relation between δ15N and animal age', *Geochimica et Cosmochimica Acta*, 48(5), pp. 1135–1140. doi: 10.1016/0016-7037(84)90204-7.

Muscatine, L. *et al.* (1984) 'Fate of photosynthetic fixed carbon in light- and shade-adapted colonies of the symbiotic coral Stylophora pistillata', *Proc. R. Soc. Lond.*, 202, pp. 181–202.

Muscatine, L., Porter, J. W. and Kaplan, I. R. (1989) 'Resource partitioning by reef corals as determined from stable isotope composition - I. δ13C of zooxanthellae and animal tissue vs depth', *Marine Biology*, 100(2), pp. 185–193. doi: 10.1007/BF00391957.

Nahon, S. *et al.* (2013) 'Spatial and temporal variations in stable carbon (δ13C) and nitrogen (δ15N) isotopic composition of symbiotic scleractinian corals', *PLoS ONE*, 8(12), pp. 1–17. doi: 10.1371/journal.pone.0081247.

Naumann, M. S. *et al.* (2009) 'Coral surface area quantification-evaluation of established techniques

by comparison with computer tomography', *Coral Reefs*, 28(1), pp. 109–117. doi: 10.1007/s00338-008-0459-3.

Oliver, T. A. and Palumbi, S. R. (2011) 'Do fluctuating temperature environments elevate coral thermal tolerance?', *Coral Reefs*, 30(2), pp. 429–440. doi: 10.1007/s00338-011-0721-y.

Osborne, A. R. and Burch, T. L. (1980) 'Internal solitons in the Andaman Sea', *Science*, 208(4443), pp. 451–460. doi: 10.1126/science.208.4443.451.

Pacherres, C. O., Schmidt, G. M. and Richter, C. (2013) 'Autotrophic and heterotrophic responses of the coral Porites lutea to large amplitude internal waves', *Journal of Experimental Biology*, 216(23), pp. 4365–4374. doi: 10.1242/jeb.085548.

Peterson, B. J. and Fry, B. (1987) 'Stable isotopes in ecosystem studies.', *Annual review of ecology and systematics. Vol. 18*, pp. 293–320. doi: 10.1146/annurev.es.18.110187.001453.

Price, J. *et al.* (2020) 'Airbrushed Coral Sample Preparation for Organic Stable Carbon and Nitrogen Isotope Analyses'. doi: 10.3354/meps08866.

Price, J. T. *et al.* (2021) 'Isotopic approaches to estimating the contribution of heterotrophic sources to Hawaiian corals', *Limnol Oceanogr*, 66, pp. 2393–2407. doi: 10.1002/lno.11760.

R Core Team (2022) 'R: A Language and Environment for Statistical Computing'. Vienna, Austria. Available at: https://www.r-project.org/.

Radice, Veronica Z *et al.* (2019) 'Evaluating coral trophic strategies using fatty acid composition and indices', pp. 1–20.

Radice, Veronica Z. *et al.* (2019) 'Upwelling as the major source of nitrogen for shallow and deep reef-building corals across an oceanic atoll system', *Functional Ecology*, 33(6), pp. 1120–1134. doi: 10.1111/1365-2435.13314.

Ramaswamy, V. *et al.* (2008) 'Distribution and sources of organic carbon , nitrogen and their isotopic signatures in sediments from the Ayeyarwady (Irrawaddy) continental shelf , northern Andaman Sea', *Marine Chemistry*, 111, pp. 137–150. doi: 10.1016/j.marchem.2008.04.006.

Reguero, B. G. *et al.* (2021) 'The value of US coral reefs for flood risk reduction', *Nature Sustainability*, 4(August). doi: 10.1038/s41893-021-00706-6.

Reid, E. C. *et al.* (2019) 'Internal waves influence the thermal and nutrient environment on a shallow coral reef', *Limnology and Oceanography*, 64(5), pp. 1949–1965. doi: 10.1002/lno.11162.

Revel, J. *et al.* (2016) 'Differential distribution of lipids in epidermis, gastrodermis and hosted

Symbiodinium in the sea anemone Anemonia viridis', *Comparative Biochemistry and Physiology -Part A : Molecular and Integrative Physiology*, 191, pp. 140–151. doi: 10.1016/j.cbpa.2015.10.017.

Richmond, R. H., Tisthammer, K. H. and Spies, N. P. (2018) 'The effects of anthropogenic stressors on reproduction and recruitment of corals and reef organisms', *Frontiers in Marine Science*. Frontiers Media S.A., p. 226. doi: 10.3389/fmars.2018.00226.

Rocker, M. M. *et al.* (2019) 'Temporal and spatial variation in fatty acid composition in Acropora tenuis corals along water quality gradients on the Great Barrier Reef, Australia', *Coral Reefs*, 38(2), pp. 215–228. doi: 10.1007/s00338-019-01768-x.

Roder, C. *et al.* (2010) 'Trophic response of Corals to large amplitude internal waves', *Marine Ecology Progress Series*, 412, pp. 113–128. doi: 10.3354/meps08707.

Roder, C. *et al.* (2011) 'Metabolic plasticity of the corals Porites lutea and Diploastrea heliopora exposed to large amplitude internal waves', pp. 57–69. doi: 10.1007/s00338-011-0722-x.

Safaie, A. *et al.* (2018) 'High frequency temperature variability reduces the risk of coral bleaching', *Nature Communications*, 9(1). doi: 10.1038/s41467-018-04074-2.

Safuan, C. D. M. *et al.* (2021) 'Physiological Response of Shallow-Water Hard Coral Acropora digitifera to Heat Stress via Fatty Acid Composition', *Frontiers in Marine Science*, 8(September), pp. 1–13. doi: 10.3389/fmars.2021.715167.

Sawall, Y. *et al.* (2014) 'Calcification , photosynthesis and nutritional status of the hermatypic coral Porites lutea : contrasting case studies from Indonesia and Thailand', pp. 1–10.

Schmidt, G. *et al.* (2012) 'Coral community composition and reef development at the Similan Islands, Andaman Sea, in response to strong environmental variations', *Marine Ecology Progress Series*, 456, pp. 113–126. doi: 10.3354/meps09682.

Schmidt, G. M. *et al.* (2016) 'Large-amplitude internal waves sustain coral health during thermal stress', *Coral Reefs*, 35(3), pp. 869–881. doi: 10.1007/s00338-016-1450-z.

Schmidt, G. M. and Richter, C. (2013) 'Coral growth and bioerosion of Porites lutea in response to large amplitude internal waves', *PLoS ONE*, 8(12). doi: 10.1371/journal.pone.0073236.

Seemann, J. *et al.* (2013) 'The use of lipids and fatty acids to measure the trophic plasticity of the coral stylophora subseriata', *Lipids*, 48(3), pp. 275–286. doi: 10.1007/s11745-012-3747-1.

Séré, M. G. *et al.* (2010) 'Journal of Experimental Marine Biology and Ecology In fl uence of heterotrophic feeding on the sexual reproduction of Pocillopora verrucosa in aquaria', *Journal of Experimental Marine Biology and Ecology*, 395(1–2), pp. 63–71. doi: 10.1016/j.jembe.2010.08.014.

Simopoulos, A. P. (2008) 'The importance of the omega-6/omega-3 fatty acid ratio in cardiovascular disease and other chronic diseases', *Experimental Biology and Medicine*, 233(6), pp. 674–688. doi: 10.3181/0711-MR-311.

Spalding, M. *et al.* (2017) 'Mapping the global value and distribution of coral reef tourism', *Marine Policy*, 82, pp. 104–113. doi: 10.1016/j.marpol.2017.05.014.

Sturaro, N. *et al.* (2021) 'Trophic plasticity of mixotrophic corals under contrasting environments', *Functional Ecology*, 35(12)(September), pp. 2841–2855. doi: 10.1111/1365-2435.13924.

Syväranta, J. *et al.* (2013) 'An Empirical Evaluation of the Utility of Convex Hull and Standard Ellipse Areas for Assessing Population Niche Widths from Stable Isotope Data', *PLoS ONE*, 8(2), pp. 1–8. doi: 10.1371/journal.pone.0056094.

Tagliafico, A. *et al.* (2017) 'Lipid-enriched diets reduce the impacts of thermal stress in corals', *Marine Ecology Progress Series*, 573, pp. 129–141.

Thibault, M. *et al.* (2022) 'Seabird-Derived Nutrients Supply Modulates the Trophic Strategies of Mixotrophic Corals', 8(January), pp. 1–12. doi: 10.3389/fmars.2021.790408.

Thibault, M., Lorrain, A. and Houlbrèque, F. (2021) 'Comment on Trophic strategy and bleaching resistance in reef-building corals', *Science Advances*, 7(23), pp. 2–5. doi: 10.1126/sciadv.abd9453.

Tolosa, I. *et al.* (2011) 'Impact of feeding and short-term temperature stress on the content and isotopic signature of fatty acids, sterols, and alcohols in the scleractinian coral Turbinaria reniformis', *Coral Reefs*, 30(3), pp. 763–774. doi: 10.1007/s00338-011-0753-3.

Torchiano, M. (2020) 'effsize: Efficient Effect Size Computation'. doi: 10.5281/zenodo.1480624.

Treignier, C. *et al.* (2008) 'Effect of light and feeding on the fatty acid and sterol composition of zooxanthellae and host tissue isolated from the scleractinian coral Turbinaria reniformis', *Limnology and Oceanography*, 53(6), pp. 2702–2710. doi: 10.4319/lo.2008.53.6.2702.

Turner, T. F., Collyer, M. L. and Krabbenhoft, T. J. (2010) 'A general hypothesis-testing framework for stable isotope ratios in ecological studies', *Ecology*, 91(8), pp. 2227–2233. doi: https://doi.org/10.1890/09-1454.1.

Vlasenko, V. and Stashchuk, N. (2007) 'Three-dimensional shoaling of large-amplitude internal waves', *Journal of Geophysical Research*, 112(C11), p. C11018. doi: 10.1029/2007JC004107.

Wall, C. B. *et al.* (2019) 'Spatial variation in the biochemical and isotopic composition of corals during bleaching and recovery', *Limnology and Oceanography*, 64(5), pp. 2011–2028. doi: 10.1002/lno.11166.

Wall, C. B. *et al.* (2020) 'Divergent symbiont communities determine the physiology and nutrition of a reef coral across a light-availability gradient', *ISME Journal*, 14(4), pp. 945–958. doi: 10.1038/s41396-019-0570-1.

Wall, M. *et al.* (2012) 'Differential Impact of Monsoon and Large Amplitude Internal Waves on Coral Reef Development in the Andaman Sea', *PLoS ONE*, 7(11). doi: 10.1371/journal.pone.0050207.

Wall, M. *et al.* (2015) 'Large-amplitude internal waves benefit corals during thermal stress', *Proceedings of the Royal Society B: Biological Sciences*, 282(1799), pp. 20–28. doi: 10.1098/rspb.2014.0650.

Wall, M., Beck, K. K., *et al.* (2023) 'Lipid biomarkers reveal trophic relationships and energetic trade-offs in contrasting phenotypes of the cold-water coral Desmophyllu m dianthus in Comau Fjord, Chile', *Functional Ecology*, (June 2022), pp. 1–17. doi: 10.1111/1365-2435.14479.

Wall, M., Doering, T., *et al.* (2023) 'Natural thermal stress-hardening of corals through cold temperature pulses in the Thai Andaman Sea'. doi: https://doi.org/10.1101/2023.06.12.544549.

Wickham, H. (2016) *ggplot2: Elegant Graphics for Data Analysis*. Springer-Verlag New York. Available at: https://ggplot2.tidyverse.org.

Wickham, H. *et al.* (2019) 'Welcome to the {tidyverse}', *Journal of Open Source Software*, 4(43), p. 1686. doi: 10.21105/joss.01686.

Williams, G. J. *et al.* (2018) 'Biophysical drivers of coral trophic depth zonation', *Marine Biology*, 165(4), pp. 1–15. doi: 10.1007/s00227-018-3314-2.

Wolanski, E. and Pickard, G. L. (1983) 'Upwelling by internal tides and kelvin waves at the continental shelf break on the great barrier reef', *Marine and Freshwater Research*, 34(1), pp. 65–80. doi: 10.1071/MF9830065.

Wyatt, A. S. J. *et al.* (2020) 'Heat accumulation on coral reefs mitigated by internal waves', *Nature Geoscience*, 13(1), pp. 28–34. doi: 10.1038/s41561-019-0486-4.

Wyatt, A. S. J. *et al.* (2023) 'Hidden heatwaves and severe coral bleaching linked to mesoscale eddies and thermocline dynamics', *Nature Communications*, 14(1), pp. 1–17. doi: 10.1038/s41467-022-35550-5.

Zhang, J. *et al.* (2023) 'Synergistic/antagonistic effects of nitrate/ammonium enrichment on fatty acid biosynthesis and translocation in coral under heat stress', *Science of the Total Environment*, 876(March), p. 162834. doi: 10.1016/j.scitotenv.2023.162834.

Zhen, X. and Wang, Y. (2015) 'An overview of methanol as an internal combustion engine fuel',

Renewable and Sustainable Energy Reviews, 52, pp. 477–493. doi: https://doi.org/10.1016/j.rser.2015.07.083.

Ziegler, M. *et al.* (2014) 'Limits to physiological plasticity of the coral Pocillopora verrucosa from the central Red Sea', pp. 1115–1129. doi: 10.1007/s00338-014-1192-8.

Supplement Figures

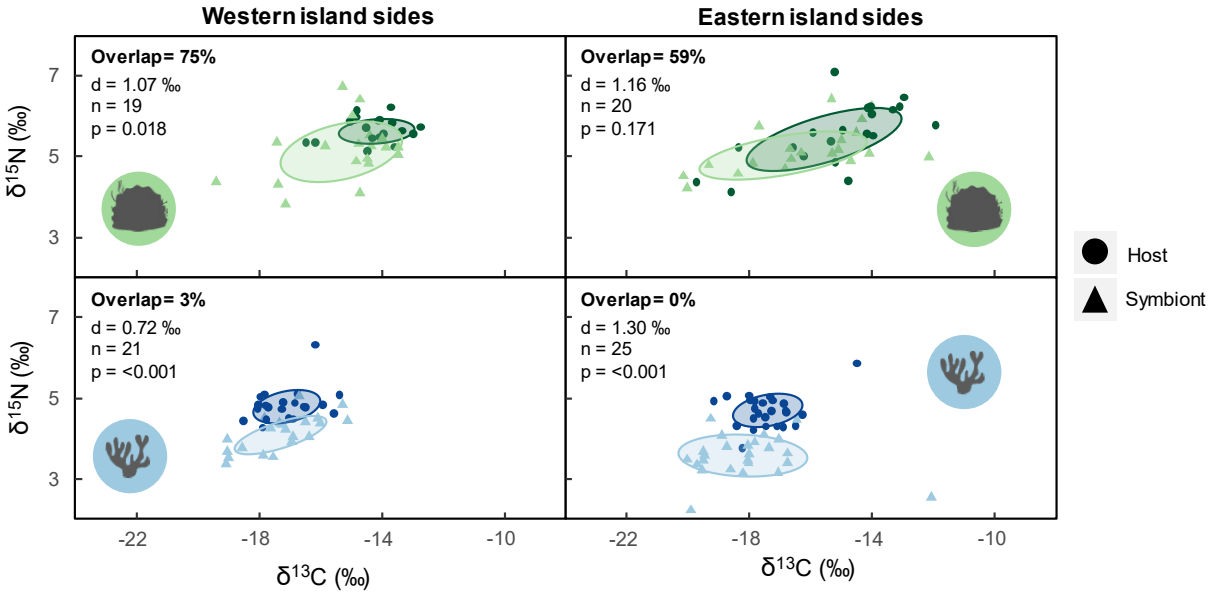

Supplement Figure 1: Isotopic biplots of corals host and symbiont at western LAIW exposed and eastern LAIW sheltered island sites. Porites host and symbiont in darker green and lighter green, respectively. Pocillopora host and symbiont in darker blue and lighter blue, respectively. 40% SIBER ellipses for host and symbiont data are fitted and their overlap as a proportion of host ellipses stated. Hoteling T^2 test were performed to analyze whether host and symbionts occupy distinct isotopic niches and p value is stated. d= Euclidean centroid distance, n=number of paired host and symbionts

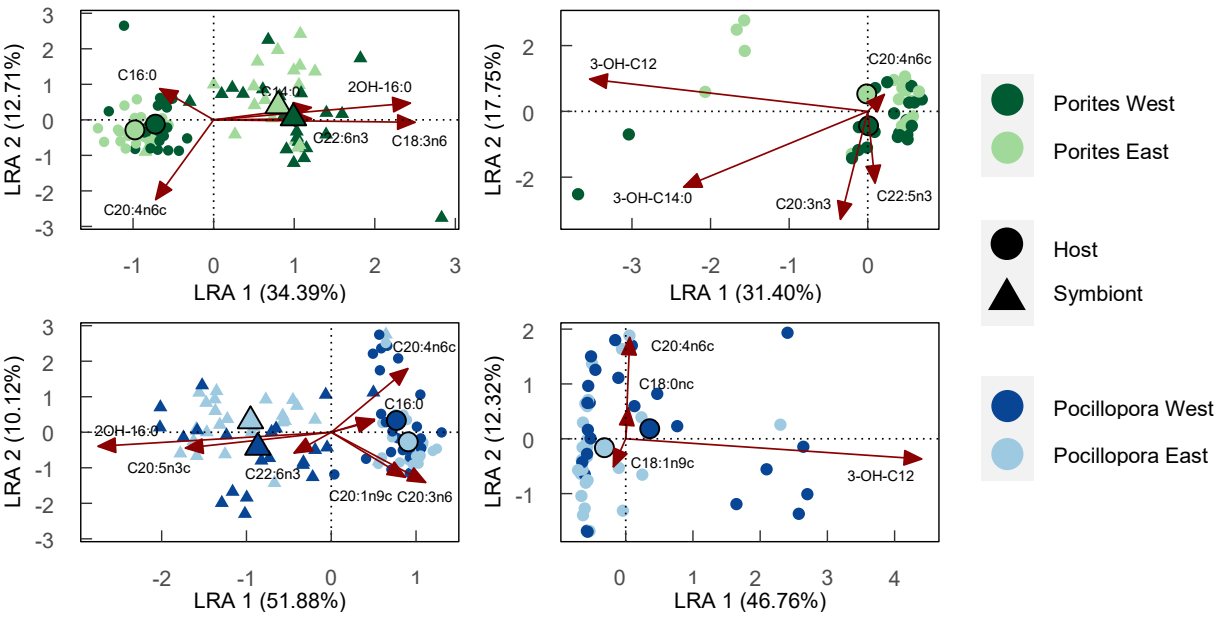

Supplement Figure 2: Log ratio analysis of all 51 fatty acid / fatty alcohols. Top Porites (green) and bottom Pocillopora (blue); left: host and symbiont together, right: host alone. Samples from LAIW exposed western and LAIW sheltered eastern island sites of Racha and Miang. Centroids of each group are indicated by larger symbols with a black outline. Components that contribute highly to the seperation are shown with an arrow indicating direction and weight of the influence.

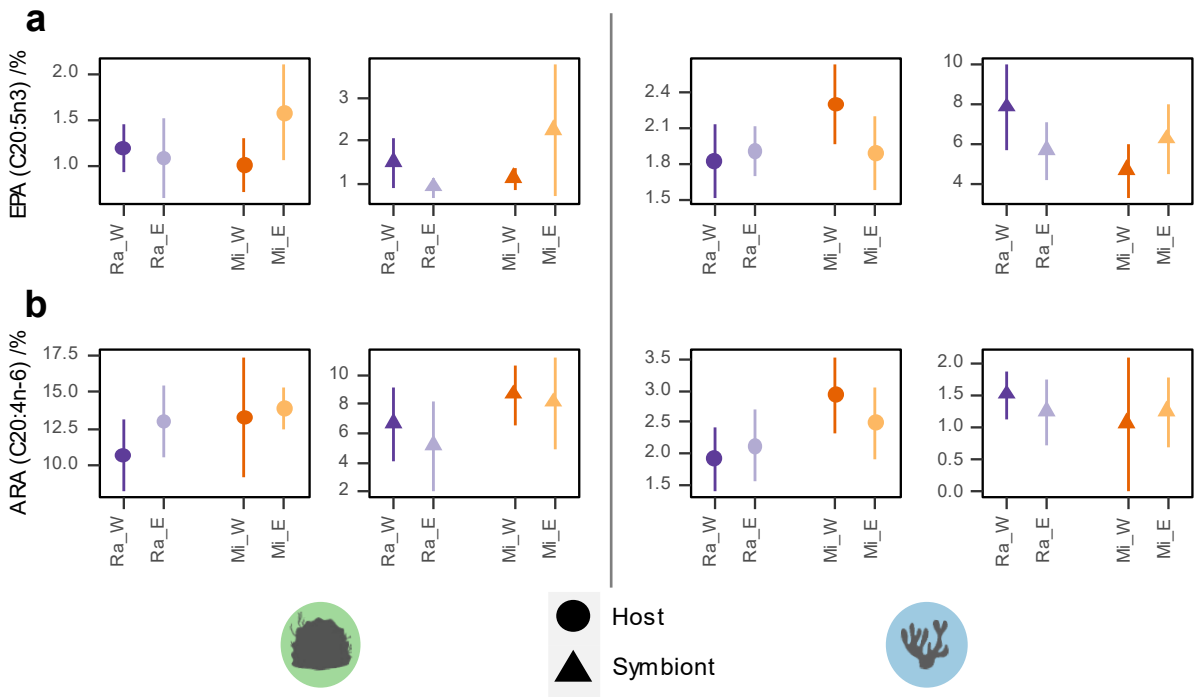

Supplement Figure 3: Mean + 95% confidence interval for relative concentration of the fatty acids (a) Eicosapentaenoic acid and (b) Arachidonic acid of separated coral host and symbiodinium fractions of Porites (left) and Pocillopora (right). Coral originated from LAIW exposed western sites (W) and LAIW sheltered eastern sites (E) of the islands Racha (Ra) and Miang (Mi) in the Andaman Sea.

Supplement tables

Supplement Table 1: Mean (SD) fatty acid per surface area (µg/cm) for separated coral host and symbiont (Symb) fractions of the corals Porites and Pocillopora. Samples originate from western (W) and eastern (E) sites of the islands Racha (Ra) and Miang (Mi) in the Andaman Sea.

FA	Pocillopora Host Mi E	Pocillopora Host Mi W	Pocillopora Host Ra E	Pocillopora Host Ra W	Porites Host Mi E	Porites Host Mi W	Porites Host Ra E	Porites Host Ra W	Pocillopora Symb Mi E	Pocillopora Symb Mi W	Pocillopora Symb Ra E	Pocillopora Symb Ra W	Porites Symb Mi E	Porites Symb Mi W	Porites Symb Ra E	Porites Symb Ra W
C4:0	0 (0)	0 (0)	0 (0)	0 (0)	0 (0)	0 (0)	0 (0)	0.01 (0.02)	0 (0)	0 (0)	0 (0)	0 (0)	0 (0)	0 (0)	0 (0)	0 (0)
C8:0	0 (0)	0.13 (0.42)	0.04 (0.15)	0.1 (0.21)	0.01 (0.04)	0.15 (0.25)	0.1 (0.16)	0.08 (0.11)	0 (0)	0.01 (0.03)	0 (0)	0 (0)	0.01 (0.01)	0.02 (0.04)	0.01 (0.01)	0.02 (0.07)
C10:0	0 (0.01)	0.03 (0.05)	0.02 (0.03)	0.02 (0.04)	0.01 (0.02)	0.03 (0.05)	0.08 (0.05)	0.04 (0.13)	0.01 (0.01)	0.01 (0.03)	0.01 (0.01)	0.02 (0.02)	0.01 (0.01)	0.02 (0.03)	0.03 (0.04)	0.02 (0.02)
C11:0	0.01 (0.03)	0 (0)	0 (0)	0.02 (0.06)	0 (0)	0 (0)	0.02 (0.06)	0.01 (0.05)	0 (0.01)	0 (0)	0 (0.01)	0 (0)	0 (0)	0 (0)	0 (0)	0 (0)
C12:0	0.2 (0.1)	0.18 (0.09)	0.19 (0.11)	0.14 (0.11)	0.03 (0.02)	0.09 (0.08)	0.1 (0.05)	0.11 (0.19)	0.1 (0.08)	0.2 (0.09)	0.12 (0.06)	0.11 (0.1)	0.04 (0.04)	0.05 (0.03)	0.07 (0.08)	0.11 (0.2)
C13:0	0.01 (0.02)	0.01 (0.02)	0.01 (0.02)	0.03 (0.03)	0 (0.01)	0.02 (0.04)	0.04 (0.07)	0.08 (0.21)	0.03 (0.02)	0.04 (0.03)	0.04 (0.04)	0.03 (0.03)	0.03 (0.03)	0.07 (0.09)	0.04 (0.06)	0.06 (0.05)
i-C15:0	0 (0)	0 (0)	0 (0)	0 (0.01)	0 (0.01)	0 (0)	0.04 (0.05)	0.03 (0.09)	0.01 (0.02)	0 (0)	0.01 (0.02)	0 (0.01)	0 (0)	0 (0.01)	0.01 (0.03)	0.01 (0.03)
C14:0	5.85 (1.89)	6.12 (2.82)	6.42 (3.61)	6.01 (4.08)	1.53 (0.66)	2.8 (1.51)	1.78 (1.26)	2.73 (1.85)	1.53 (0.4)	5.47 (2.84)	2.93 (1.49)	2.63 (3.65)	1.08 (0.85)	2.41 (1.32)	1.47 (1.33)	2.9 (5.58)
C14:1	0.15 (0.04)	0.12 (0.07)	0.13 (0.07)	0.13 (0.11)	0.07 (0.06)	0.05 (0.06)	0.03 (0.05)	0.13 (0.09)	0.07 (0.02)	0.12 (0.11)	0.09 (0.05)	0.17 (0.21)	0.12 (0.1)	0.19 (0.1)	0.1 (0.07)	0.2 (0.18)
2OH-C10:0	0.02 (0.04)	0 (0)	0 (0.01)	0 (0)	0 (0)	0 (0)	0.03 (0.09)	0.12 (0.3)	0.01 (0.04)	0.05 (0.08)	0 (0.01)	0 (0.01)	0 (0)	0 (0)	0 (0)	0.03 (0.06)
i-16:0	0 (0)	0 (0)	0 (0.01)	0 (0)	0.01 (0.02)	0.08 (0.12)	0 (0)	0.02 (0.07)	0.01 (0.01)	0 (0)	0 (0)	0 (0)	0 (0)	0.01 (0.02)	0.01 (0.02)	0.02 (0.03)
C15:0	0.06 (0.04)	0.05 (0.04)	0.06 (0.04)	0.06 (0.06)	0.17 (0.06)	0.55 (0.33)	0.25 (0.25)	0.54 (0.56)	0.02 (0.02)	0.02 (0.02)	0.03 (0.02)	0.04 (0.06)	0.06 (0.07)	0.14 (0.13)	0.07 (0.06)	0.12 (0.09)
C15:1	0.22 (0.4)	0.4 (0.52)	0.08 (0.16)	0.2 (0.25)	0.13 (0.2)	1.01 (1.54)	0.35 (0.47)	0.12 (0.31)	0.04 (0.08)	0.01 (0.03)	0.03 (0.05)	0.14 (0.23)	0.02 (0.03)	0.02 (0.05)	0.05 (0.08)	0.08 (0.1)
i-17:0	0.18 (0.18)	0.29 (0.35)	0.23 (0.26)	0.22 (0.29)	0.15 (0.24)	0.29 (0.52)	0.09 (0.2)	0.48 (0.71)	0.04 (0.1)	0.01 (0.03)	0.05 (0.11)	0.03 (0.05)	0.03 (0.04)	0.04 (0.06)	0.04 (0.07)	0.07 (0.1)

FA	Pocillopora Host Mi E	Pocillopora Host Mi W	Pocillopora Host Ra E	Pocillopora Host Ra W	Porites Host Mi E	Porites Host Mi W	Porites Host Ra E	Porites Host Ra W	Pocillopora Symb Mi E	Pocillopora Symb Mi W	Pocillopora Symb Ra E	Pocillopora Symb Ra W	Porites Symb Mi E	Porites Symb Mi W	Porites Symb Ra E	Porites Symb Ra W
2-OH-C12:0	0 (0.01)	0.04 (0.15)	0.01 (0.05)	0.05 (0.14)	0.02 (0.04)	0.03 (0.08)	0.08 (0.23)	0.01 (0.03)	0.14 (0.12)	0.2 (0.19)	0.19 (0.22)	0.14 (0.16)	0.19 (0.18)	0.19 (0.32)	0.09 (0.2)	0.27 (0.35)
C16:0	51.77 (15.03)	53.71 (27.33)	55.44 (31.29)	54.85 (35.74)	53.89 (20.47)	92.21 (47.43)	60.32 (40.78)	97.77 (69.84)	7.31 (4.4)	29.58 (22.47)	14.54 (9.36)	14.68 (26.61)	14.15 (12.87)	19.96 (15.82)	18.54 (15.04)	22.58 (23.93)
C16:1	2.88 (1.45)	3.4 (1.94)	3.3 (1.88)	3.56 (2.75)	0.54 (0.19)	0.42 (0.31)	1.81 (3.36)	2.44 (4.47)	0.68 (0.2)	2.48 (1.39)	1.33 (0.88)	1.5 (2.12)	0.25 (0.28)	0.47 (0.51)	0.41 (0.31)	1.11 (2.36)
a-17:0	0.15 (0.28)	0 (0)	0.02 (0.06)	0.01 (0.05)	0.13 (0.28)	0 (0)	0.07 (0.24)	0.42 (1.32)	0.07 (0.2)	0 (0)	0 (0.01)	0.01 (0.04)	0 (0)	0 (0)	0 (0)	0.07 (0.15)
C16:2n4	0.04 (0.14)	0.03 (0.05)	0.02 (0.06)	0.14 (0.48)	0.07 (0.14)	0.26 (0.51)	0 (0)	0.21 (0.56)	0 (0)	0 (0)	0 (0.01)	0 (0)	0 (0)	0 (0)	0 (0)	0 (0)
cis-9-10-C17:0	0 (0.01)	0 (0)	0.02 (0.05)	0.03 (0.07)	0.29 (0.32)	0.52 (0.6)	0.33 (0.88)	0.77 (1.41)	0 (0)	0.05 (0.07)	0 (0)	0.07 (0.11)	0.09 (0.05)	0.13 (0.11)	0.03 (0.06)	0.06 (0.08)
C17:0	0.06 (0.08)	0.04 (0.06)	0.07 (0.09)	0.09 (0.14)	0.05 (0.07)	0.07 (0.15)	0.1 (0.11)	0.2 (0.16)	0.07 (0.03)	0.06 (0.06)	0.06 (0.06)	0.06 (0.05)	0.03 (0.03)	0.02 (0.04)	0.04 (0.05)	0.05 (0.05)
C17:1	0.02 (0.05)	6.56 (14.7)	0.57 (2.1)	2.93 (9.32)	0 (0)	21.09 (44.93)	1.77 (2.85)	0 (0.01)	0.12 (0.14)	0.13 (0.12)	0.17 (0.16)	0.19 (0.3)	0 (0)	0.16 (0.4)	0.12 (0.22)	0.06 (0.13)
C16:3n4	1.78 (2.2)	1.48 (2.29)	2.17 (2.76)	7.13 (17.02)	1.88 (2.08)	4.5 (5.7)	2.59 (2.99)	2.22 (2.89)	0.16 (0.14)	0.74 (0.76)	0.23 (0.33)	0.24 (0.31)	0.42 (0.53)	0.92 (0.95)	0.48 (0.94)	0.68 (0.61)
2-OH-14:0	0 (0)	0.84 (2.92)	0 (0.01)	0.33 (1.16)	0 (0)	0 (0)	0 (0)	0 (0)	0 (0)	0 (0)	0 (0.02)	0 (0)	0 (0)	0 (0)	0 (0)	0 (0)
C18:0nc	19.24 (4.45)	22.93 (9.1)	19.28 (8.58)	24.48 (15.06)	15.15 (4.79)	24.34 (12.28)	17.68 (8.59)	28.87 (20.09)	2.67 (1.11)	10 (6.55)	4.77 (2.5)	5.62 (9.3)	5.88 (2.61)	8.76 (4.67)	7.54 (4.73)	9.77 (10.38)
C18:1n9t	0 (0)	0 (0)	0 (0)	0 (0)	0 (0)	0 (0)	0 (0)	0.11 (0.41)	0.02 (0.05)	0 (0)	0.01 (0.04)	0 (0)	0 (0.01)	0 (0)	0.01 (0.03)	0.02 (0.06)
C18:1n9c	9.73 (3.76)	9.46 (5.64)	9.56 (5.43)	11.4 (8.99)	17.53 (10.02)	32.72 (21.52)	15.97 (10.35)	27.95 (17.04)	1.07 (0.6)	5.31 (3.4)	2.09 (1.53)	2.38 (3.56)	3.7 (4.07)	8.22 (6.33)	4.19 (2.81)	7.2 (4.61)
C18:1n7c	0.87 (0.33)	0.95 (0.5)	0.9 (0.43)	1.02 (0.69)	0.36 (0.2)	0.9 (0.51)	0.31 (0.16)	0.68 (0.47)	0.08 (0.04)	0.38 (0.27)	0.17 (0.16)	0.25 (0.47)	0.09 (0.07)	0.2 (0.16)	0.06 (0.05)	0.26 (0.45)
C18:2n6t	0.33 (0.6)	0 (0)	0.03 (0.11)	0 (0)	0.13 (0.25)	0.24 (0.72)	0.09 (0.28)	1.17 (3.39)	0.12 (0.39)	0 (0)	0 (0)	0.02 (0.05)	0.14 (0.32)	0 (0)	0 (0.01)	0.1 (0.24)
C18:2n6c	2.25 (1.38)	1.95 (1.02)	1.65 (0.92)	1.97 (1.36)	1.84 (1.49)	3.14 (3.47)	1.85 (2.17)	2.58 (1.97)	0.35 (0.1)	1.48 (0.96)	0.64 (0.27)	0.66 (0.87)	0.8 (1)	1.39 (1.19)	0.72 (0.66)	1.18 (1.02)
cis9,10 C19:0	0 (0)	0 (0)	0 (0)	0.03 (0.09)	0 (0)	0.26 (0.77)	0 (0)	0.01 (0.02)	0 (0)	0 (0)	0 (0)	0 (0)	0 (0)	0 (0)	0 (0)	0 (0)
C18:3n6	2.78 (1.51)	2.81 (1.87)	2.75 (1.68)	3.12 (2.56)	2.16 (1.63)	5.76 (4.07)	2.77 (2.36)	6.27 (4.2)	0.67 (0.38)	3.09 (1.52)	1.33 (0.62)	1.26 (1.7)	3.99 (2.79)	9.7 (6.82)	4.57 (4.16)	6.91 (4.33)

FA	Pocillopora Host Mi E	Pocillopora Host Mi W	Pocillopora Host Ra E	Pocillopora Host Ra W	Porites Host Mi E	Porites Host Mi W	Porites Host Ra E	Porites Host Ra W	Pocillopora Symb Mi E	Pocillopora Symb Mi W	Pocillopora Symb Ra E	Pocillopora Symb Ra W	Porites Symb Mi E	Porites Symb Mi W	Porites Symb Ra E	Porites Symb Ra W
3-OH-C14:0	0.05 (0.08)	0.05 (0.11)	0.02 (0.04)	0.02 (0.04)	1.17 (3.32)	5.85 (10.96)	0.25 (0.82)	0.93 (1.9)	0.01 (0.02)	0.01 (0.01)	0 (0)	0.1 (0.26)	0 (0)	0.66 (1.86)	0.13 (0.25)	0.59 (2.14)
C18:3n3	0.65 (0.61)	0.3 (0.2)	0.29 (0.19)	0.29 (0.29)	0.83 (1)	2.08 (3.32)	1 (0.84)	1.09 (0.97)	0.13 (0.1)	0.3 (0.21)	0.16 (0.07)	0.14 (0.1)	0.12 (0.18)	0.21 (0.31)	0.07 (0.14)	0.24 (0.27)
2OH-16:0	2.28 (0.82)	2.39 (1.48)	2.42 (1.4)	3.93 (2.75)	0.83 (0.5)	1.77 (0.87)	0.99 (0.7)	2.1 (1.56)	2.91 (0.94)	6.79 (3.21)	4.22 (2.58)	6.82 (6.6)	1.74 (1.53)	3.88 (2.47)	1.64 (1.64)	4.01 (5.17)
C20:0	2.66 (0.89)	3.31 (1.48)	2.85 (1.59)	3.33 (2.13)	0.67 (0.28)	1.21 (1.04)	0.61 (0.38)	1.33 (1.01)	0.22 (0.12)	1.54 (1.16)	0.48 (0.34)	0.73 (1.4)	0.2 (0.11)	0.35 (0.27)	0.21 (0.14)	0.77 (1.89)
C20:1n9c	4.02 (1.77)	4.28 (2.3)	4.15 (2.73)	4.85 (3.71)	1.87 (1.01)	3.57 (2.94)	1.42 (1.2)	2.34 (1.91)	0.31 (0.22)	2.24 (1.82)	0.68 (0.69)	1.13 (2.44)	0.43 (0.41)	0.73 (0.57)	0.39 (0.37)	1.14 (2.46)
C20:2n6c	1.85 (1.27)	1.39 (0.57)	1.38 (0.57)	2.11 (2.04)	2.23 (1.31)	3.3 (3.19)	1.89 (1.62)	2.68 (1.83)	0.13 (0.05)	0.64 (0.47)	0.23 (0.17)	0.3 (0.42)	0.48 (0.41)	0.78 (0.67)	0.29 (0.23)	0.64 (0.69)
C20:3n6	6.35 (2.66)	6.19 (3.64)	6.31 (3.79)	7.95 (6.28)	1.39 (1.18)	3.99 (3.25)	1.39 (0.96)	2.27 (1.58)	0.49 (0.33)	3.45 (2.63)	1.01 (0.9)	1.46 (2.34)	0.31 (0.26)	0.7 (0.69)	0.17 (0.17)	1.09 (2.95)
C20:4n6c	3.26 (1.11)	4.07 (1.47)	2.75 (1.18)	3.02 (2.35)	18.43 (6.16)	32.53 (18.02)	16.37 (7.38)	22 (10.74)	0.29 (0.18)	0.63 (0.47)	0.53 (0.39)	0.75 (1.07)	3.76 (3.02)	6.27 (3.52)	2.1 (1.78)	4.06 (4.09)
C20:3n3	0.33 (0.32)	0.08 (0.04)	0.14 (0.2)	0.08 (0.13)	0.24 (0.39)	4.53 (11.54)	0.14 (0.3)	0.23 (0.2)	0.1 (0.29)	0.02 (0.03)	0.02 (0.04)	0.04 (0.06)	0.03 (0.07)	0.01 (0.03)	0.09 (0.21)	0.12 (0.16)
C20:4n3	0.1 (0.17)	0.01 (0.03)	0.07 (0.24)	0.19 (0.42)	0.08 (0.22)	0 (0)	0.01 (0.03)	1.49 (4.07)	0 (0)	0.01 (0.02)	0 (0)	0.02 (0.07)	0 (0)	0 (0)	0 (0)	0 (0)
C22:0	0.51 (0.23)	0.64 (0.22)	0.4 (0.19)	0.64 (0.41)	0.37 (0.16)	0.57 (0.32)	0.36 (0.25)	0.83 (0.7)	0.07 (0.03)	0.25 (0.15)	0.1 (0.06)	0.13 (0.23)	0.19 (0.19)	0.17 (0.14)	0.12 (0.09)	0.25 (0.34)
C20:5n3c	2.63 (0.97)	3.4 (1.59)	2.62 (1.26)	3.14 (2.34)	2.32 (1.52)	2.68 (1.87)	1.6 (1.44)	3.06 (3.02)	1.41 (0.52)	3.84 (1.77)	2.37 (1.42)	3.68 (4.18)	1.1 (1.08)	0.93 (0.76)	0.45 (0.41)	1.68 (3.25)
C22:1n9c	0.21 (0.09)	0.26 (0.15)	0.23 (0.16)	0.36 (0.21)	0.35 (0.15)	0.55 (0.45)	0.22 (0.21)	0.39 (0.27)	0.04 (0.04)	0.15 (0.09)	0.07 (0.08)	0.11 (0.14)	0.15 (0.09)	0.1 (0.08)	0.19 (0.23)	0.16 (0.15)
C22: 2n6c	0.05 (0.06)	0.01 (0.02)	0.02 (0.03)	0.02 (0.06)	0.05 (0.07)	0.08 (0.12)	0.04 (0.08)	0.08 (0.09)	0.01 (0.03)	0 (0.01)	0 (0.01)	0.01 (0.02)	0 (0)	0.01 (0.02)	0.02 (0.04)	0.01 (0.03)
C23:0	0.06 (0.06)	0.06 (0.11)	0.07 (0.12)	0.04 (0.07)	0.28 (0.6)	0.11 (0.08)	0.04 (0.05)	0.16 (0.21)	0.06 (0.1)	0.02 (0.03)	0.03 (0.06)	0.08 (0.22)	0.08 (0.17)	0.02 (0.03)	0.02 (0.02)	0.05 (0.06)
C24:0	0.28 (0.13)	0.38 (0.23)	0.25 (0.2)	0.48 (0.41)	0.33 (0.14)	0.73 (0.42)	0.37 (0.34)	0.56 (0.46)	0.03 (0.04)	0.12 (0.13)	0.06 (0.05)	0.29 (0.69)	0.07 (0.07)	0.1 (0.1)	0.22 (0.39)	0.12 (0.11)
C22:5n3	1.32 (0.49)	1.44 (0.64)	1.21 (0.75)	1.93 (1.32)	2.83 (2.98)	6.64 (5.99)	1.88 (2.79)	4.18 (3.83)	0.16 (0.16)	0.45 (0.34)	0.15 (0.14)	0.37 (0.62)	0.67 (0.96)	1.65 (1.76)	0.29 (0.39)	0.78 (0.68)
C22:6n3	12.83 (5.63)	12.87 (7.94)	11.76 (6.91)	14.57 (10.87)	5.51 (3.42)	8.93 (5.89)	3.24 (1.62)	10.55 (9.05)	2.75 (1.06)	9.99 (5.56)	4.4 (2.34)	5.26 (7.15)	3.47 (2.47)	6.9 (3.94)	2.92 (2.47)	6.43 (8.46)

Supplement Table 2: Number of samples per analysis type. Type = Symbiotic partner faction

Species	Type	Island	Site	n (FA analyses)	n (SI analyses)	n (AFDM measurement)
Pocillopora	Host	Miang	East	11	9	11
Pocillopora	Host	Miang	West	12	12	12
Pocillopora	Host	Racha	East	16	16	15
Pocillopora	Host	Racha	West	12	9	11
Porites	Host	Miang	East	8	8	8
Porites	Host	Miang	West	9	7	9
Porites	Host	Racha	East	11	12	12
Porites	Host	Racha	West	14	11	13
Pocillopora	Symb	Miang	East	11	9	10
Pocillopora	Symb	Miang	West	11	12	12
Pocillopora	Symb	Racha	East	15	16	15
Pocillopora	Symb	Racha	West	10	9	10
Porites	Symb	Miang	East	7	8	8
Porites	Symb	Miang	West	8	7	9
Porites	Symb	Racha	East	11	12	11
Porites	Symb	Racha	West	13	11	10

Supplement Table 3: Mean and standard deviation of stable isotope data taken from separated coral hosts and symbionts from Pocillopora verrucosa and Porites lutea. Samples were taken from eastern and western sites of the islands Racha and Miang in the Andaman Sea.

Species	Island	Site	$\delta^{13}C_{Host}$ (‰)	$\delta^{13}C_{Symbiont}$ (‰)	$\delta^{13}C_{H-S}$ (‰)	$\delta^{15}N_{Host}$ (‰)	$\delta^{15}N_{Symbiont}$ (‰)	$\delta^{15}N_{H-S}$ (‰)
Pocillopora	pooled	East	-17.41 (0.91)	-18.07 (1.66)	0.66 (1.97)	4.66 (0.41)	3.54 (0.51)	1.12 (0.71)
		West	-17.11 (0.88)	-17.28 (1.20)	0.17 (0.51)	4.82 (0.41)	4.12 (0.45)	0.70 (0.58)
	Miang	East	-17.42 (0.64)	-18.50 (1.25)	1.08 (1.02)	4.34 (0.31)	3.45 (0.28)	0.90 (0.27)
		West	-16.65 (0.80)	-16.59 (0.88)	-0.06 (0.36)	4.82 (0.53)	4.36 (0.37)	0.47 (0.63)
	Racha	East	-17.40 (1.06)	-17.82 (1.85)	0.43 (2.34)	4.84 (0.35)	3.60 (0.61)	1.25 (0.85)
		West	-17.71 (0.58)	-18.20 (0.92)	0.49 (0.53)	4.81 (0.19)	3.80 (0.35)	1.01 (0.31)
Porites	pooled	East	-15.10 (2.00)	-16.20 (2.17)	1.09 (1.56)	5.55 (0.77)	5.16 (0.57)	0.39 (0.78)
		West	-14.25 (0.97)	-15.08 (1.54)	0.83 (1.22)	5.66 (0.30)	5.23 (0.67)	0.43 (0.61)
	Miang	East	-13.55 (0.98)	-14.33 (1.03)	0.77 (0.51)	6.18 (0.47)	5.55 (0.57)	0.63 (0.44)
		West	-13.99 (0.29)	-14.18 (0.47)	0.19 (0.39)	5.79 (0.24)	5.08 (0.23)	0.71 (0.24)
	Racha	East	-16.14 (1.83)	-17.45 (1.79)	1.31 (1.98)	5.12 (0.62)	4.89 (0.41)	0.23 (0.93)
		West	-14.41 (1.21)	-15.65 (1.73)	1.23 (1.40)	5.57 (0.32)	5.32 (0.85)	0.26 (0.72)

Supplement Table 4: Statistical models (GLMs and ANOVAs) for differences in putative health markers of separated coral host and symbiont fractions of Pocillopora and Porites. Site with two levels LAIW exposed west and LAIW sheltered east. Island with two levels Racha and Miang. Significant values in bold (p<0.05).

DV	Species	Faction	Test	Factor	Sum Sq	Df	F value/ LR Chisq	p-value
AFDM/surface (mg/cm2)	Pocillopora	Host	GLM (Inv. Gaus.)	Island		1	0.048	0.826
				Site		1	3.236	0.072
				Island:Site		1	0.619	0.431
		Symbiont	GLM (Gamma)	Island		1	0.227	0.634
				Site		1	1.376	0.241
				Island:Site		1	1.249	0.264
	Porites	Host	GLM (Inv. Gaus.)	Island		1	0.318	0.573
				Site		1	3.952	**0.047**
				Island:Site		1	0.66	0.417
		Symbiont	GLM (Gamma)	Island		1	0.543	0.461
				Site		1	4.843	**0.028**
				Island:Site		1	0.156	0.693
EPA : ARA	Pocillopora	Host	GLM (Inv. Gaus.)	Island		1	2.671	0.102
				Site		1	0.508	0.476
				Island:Site		1	0.192	0.661
		Symbiont	GLM (Gamma)	Island		1	0	0.984
				Site		1	0.896	0.344
				Island:Site		1	1.119	0.29
	Porites	Host	GLM (Inv. Gaus.)	Island		1	0.218	0.64
				Site		1	0.009	0.924
				Island:Site		1	4.367	**0.037**
		Symbiont	GLM (Inv. Gaus.)	Island		1	4.216	**0.04**
				Site		1	1.093	0.296
				Island:Site		1	4.111	**0.043**
PUFA n-3 : n-6	Pocillopora	Host	ANOVA	(Intercept)	57.35	1	1628.514	**<0.001**
				Island	0.00	1	0.095	0.759
				Site	0.02	1	0.439	0.511
				Island:Site	0.00	1	0.023	0.879
				Residuals	1.66	47		
		Symbiont	ANOVA	(Intercept)	198.35	1	503.64	**<0.001**
				Island	0.13	1	0.327	0.57
				Site	0.39	1	0.978	0.328
				Island:Site	2.45	1	6.216	**0.017**
				Residuals	16.94	43		
	Porites	Host	GLM (Inv. Gaus.)	Island		1	2.312	0.128
				Site		1	8.583	**0.003**
				Island:Site		1	0.307	0.579
		Symbiont	ANOVA	(Intercept)	10.49	1	126.415	**<0.001**
				Island	0.00	1	0.044	0.835
				Site	0.01	1	0.064	0.801
				Island:Site	0.02	1	0.217	0.644
				Residuals	2.90	35		
PUFA /%	Pocillopora	Host	ANOVA	(Intercept)	31311.62	1	2477.072	**<0.001**
				Island	9.39	1	0.743	0.393
				Site	4.10	1	0.325	0.572
				Island:Site	30.14	1	2.384	0.129
				Residuals	594.11	47		

DV	Species	Faction	Test	Factor	Sum Sq	Df	F value/ LR Chisq	p-value
PUFA /%	Pocillopora	Symbiont	ANOVA	(Intercept)	35239.78	1	1294.926	**<0.001**
				Island	22.63	1	0.831	0.367
				Site	21.57	1	0.793	0.378
				Island:Site	25.85	1	0.95	0.335
				Residuals	1170.19	43		
	Porites	Host	ANOVA	(Intercept)	32213.08	1	1529.811	**<0.001**
				Island	126.97	1	6.03	**0.019**
				Site	25.87	1	1.228	0.275
				Island:Site	0.15	1	0.007	0.934
				Residuals	800.16	38		
		Symbiont	GLM (Inv. Gaus.)	Island		1	7.238	**0.007**
				Site		1	8.41	**0.004**
				Island:Site		1	1.075	0.3

Supplement Table 5: Results of post hoc estimated marginal means with Tukey HSD correction for health markers. Models for separated Pocillopora and Porites host and symbiont fractions. Significant values (p<0.05) in bold. Mi = Miang, Ra = Racha.

DV	Species	Faction	contrast	estimate	SE	df	t-ratio / z-ratio	p-value
AFDM / surface	Pocillopora	Symbiont	Mi E - Ra E	-0.54	0.34	43	-1.589	0.396
			Mi E - Mi W	-0.756	0.463	43	-1.633	0.371
			Mi E - Ra W	-0.541	0.407	43	-1.331	0.549
			Ra E - Mi W	-0.216	0.545	43	-0.397	0.978
			Ra E - Ra W	-0.001	0.497	43	-0.003	1
			Mi W - Ra W	0.215	0.589	43	0.366	0.983
	Porites	Host	Mi E - Ra E	-0.012	0.016	Inf	-0.749	0.877
			Mi E - Mi W	0.009	0.012	Inf	0.739	0.881
			Mi E - Ra W	0.011	0.011	Inf	0.99	0.755
			Ra E - Mi W	0.021	0.014	Inf	1.517	0.427
			Ra E - Ra W	0.023	0.013	Inf	1.763	0.291
			Mi W - Ra W	0.002	0.007	Inf	0.31	0.99
		Symbiont	Mi E - Ra E	0.143	0.127	34	1.13	0.674
			Mi E - Mi W	-0.216	0.2	34	-1.08	0.704
			Mi E - Ra W	-0.173	0.184	34	-0.942	0.782
			Ra E - Mi W	-0.36	0.176	34	-2.041	0.193
			Ra E - Ra W	-0.317	0.158	34	-2.01	0.204
			Mi W - Ra W	0.043	0.221	34	0.193	0.997
EPA : ARA	Pocillopora	Host	Mi E - Ra E	-0.042	0.021	Inf	-1.975	0.197
			Mi E - Mi W	-0.048	0.024	Inf	-1.999	0.188
			Mi E - Ra W	-0.03	0.022	Inf	-1.395	0.503
			Ra E - Mi W	-0.006	0.026	Inf	-0.244	0.995
			Ra E - Ra W	0.011	0.024	Inf	0.47	0.966
			Mi W - Ra W	0.018	0.027	Inf	0.664	0.911
	Porites	Host	Mi E - Ra E	-51.636	46.168	Inf	-1.118	0.678
			Mi E - Mi W	-70.306	52.833	Inf	-1.331	0.543
			Mi E - Ra W	12.301	34.312	Inf	0.358	0.984

DV	Species	Faction	contrast	estimate	SE	df	t-ratio / z-ratio	p-value
EPA : ARA	Porites	Host	Ra E - Mi W	-18.67	57.3	Inf	-0.326	0.988
			Ra E - Ra W	63.937	40.857	Inf	1.565	0.399
			Mi W - Ra W	82.606	48.261	Inf	1.712	0.317
		Symbiont	Mi E - Ra E	-0.736	13.055	Inf	-0.056	1
			Mi E - Mi W	-40.72	28.498	Inf	-1.429	0.481
			Mi E - Ra W	11.058	10.25	Inf	1.079	0.702
			Ra E - Mi W	-39.984	27.942	Inf	-1.431	0.48
			Ra E - Ra W	11.794	8.584	Inf	1.374	0.516
			Mi W - Ra W	51.778	26.747	Inf	1.936	0.213
Percent PUFA	Porites	Host	Mi E - Ra E	3.677	2.132	38	1.724	0.326
			Mi E - Mi W	-1.485	2.23	38	-0.666	0.909
			Mi E - Ra W	1.951	2.034	38	0.959	0.773
			Ra E - Mi W	-5.161	2.063	38	-2.503	0.076
			Ra E - Ra W	-1.726	1.849	38	-0.933	0.787
			Mi W - Ra W	3.436	1.961	38	1.753	0.312
		Symbiont	Mi E - Ra E	-0.001	0	Inf	-2.235	0.114
			Mi E - Mi W	0	0	Inf	1.344	0.535
			Mi E - Ra W	0	0	Inf	0.085	1
			Ra E - Mi W	0.001	0	Inf	3.724	**0.001**
			Ra E - Ra W	0.001	0	Inf	2.577	**0.049**
			Mi W - Ra W	0	0	Inf	-1.527	0.421
PUFA n-3 : n-6	Pocillopora	Symbiont	Mi E - Ra E	0.356	0.249	43	1.428	0.489
			Mi E - Mi W	0.645	0.268	43	2.411	0.09
			Mi E - Ra W	0.077	0.274	43	0.282	0.992
			Ra E - Mi W	0.289	0.249	43	1.161	0.654
			Ra E - Ra W	-0.279	0.256	43	-1.087	0.699
			Mi W - Ra W	-0.568	0.274	43	-2.071	0.179
	Porites	Host	Mi E - Ra E	-5.339	4.962	Inf	-1.076	0.704
			Mi E - Mi W	5.027	2.979	Inf	1.687	0.33
			Mi E - Ra W	2.553	3.242	Inf	0.787	0.86
			Ra E - Mi W	10.365	4.073	Inf	2.545	0.053
			Ra E - Ra W	7.891	4.27	Inf	1.848	0.251
			Mi W - Ra W	-2.474	1.577	Inf	-1.569	0.396

Supplement Table 6: Model output (GLM and ANOVA) for differences in putative trophic markers of separated coral host and symbiont fractions of Pocillopora and Porites. Site with two levels LAIW exposed west and LAIW sheltered east. Island with two levels Racha and Miang. Significant values in bold (p<0.05).

DV	Species	Faction	Test		Sum Sq	Df	F value/ LR Chisq	p-value
Animal derived FA : PS derived FA	Pocillopora	Host	GLM (Inv. Gaus.)	Island		1	0.484	0.486
				Site		1	1.176	0.278
				Island:Site		1	3.068	0.08
		Symbiont	GLM (Gamma)	Island		1	0.36	0.549
				Site		1	0.398	0.528
				Island:Site		1	2.739	0.098
	Porites	Host	ANOVA	(Intercept)	15801.65	1	225.291	**<0.001**
				Island	541.01	1	7.713	**0.008**
				Site	285.08	1	4.065	0.051
				Island:Site	0.09	1	0.001	0.972
				Residuals	2665.27	38		
		Symbiont	GLM (Inv. Gaus.)	Island		1	0.451	0.502
				Site		1	0.033	0.856
				Island:Site		1	0.74	0.39
C18:1n-9 : C18:1n-7	Pocillopora	Host	ANOVA	(Intercept)	5945.02	1	809.732	**<0.001**
				Island	0.15	1	0.021	0.886
				Site	1.90	1	0.259	0.613
				Island:Site	11.09	1	1.511	0.225
				Residuals	345.07	47		
		Symbiont	ANOVA	(Intercept)	12311.19	1	43.473	**<0.001**
				Island	263.38	1	0.93	0.34
				Site	155.69	1	0.55	0.462
				Island:Site	288.50	1	1.019	0.318
				Residuals	12177.31	43		
	Porites	Host	ANOVA	(Intercept)	84670.8	1	308.369	**<0.001**
				Island	352.3	1	1.283	0.264
				Site	831.3	1	3.028	0.09
				Island:Site	90.7	1	0.33	0.569
				Residuals	10433.9	38		
		Symbiont	ANOVA	(Intercept)	368504	1	7.196	**0.011**
				Island	93671	1	1.829	0.185
				Site	75686	1	1.478	0.232
				Island:Site	74436	1	1.454	0.236
				Residuals	1792230	35		
EPA : DHA	Pocillopora	Host	ANOVA	(Intercept)	2.89	1	595.549	**<0.001**
				Island	0.01	1	1.24	0.271
				Site	0.00	1	0.879	0.353
				Island:Site	0.02	1	4.202	**0.046**
				Residuals	0.23	47		

DV	Species	Faction	Test		Sum Sq	Df	F value/ LR Chisq	p-value
EPA : DHA	Pocillopora	Symbiont	ANOVA	(Intercept)	14.25	1	408.079	**<0.001**
				Island	0.42	1	11.899	**0.001**
				Site	0.02	1	0.617	0.437
				Island:Site	0.34	1	9.853	**0.003**
				Residuals	1.50	43		
	Porites	Host	GLM (Gamma)	Island		1	0.227	0.634
				Site		1	5.17	**0.023**
				Island:Site		1	0.118	0.731
		Symbiont	GLM (Gamma)	Island		1	0.2	0.655
				Site		1	5.855	**0.016**
				Island:Site		1	9.76	**0.002**
Total fa per surface area	Pocillopora	Host	GLM (Gamma)	Island		1	0.085	0.771
				Site		1	0.777	0.378
				Island:Site		1	0.038	0.846
		Symbiont	ANOVA	(Intercept)	125881.4	1	62.057	**<0.001**
				Island	1073.8	1	0.529	0.471
				Site	15579.1	1	7.68	**0.008**
				Island:Site	9352.8	1	4.611	**0.037**
				Residuals	87225.3	43		
	Porites	Host	GLM (Inv. Gaus.)	Island		1	0.003	0.955
				Site		1	10.652	**0.001**
				Island:Site		1	0.107	0.744
		Symbiont	GLM (Inv. Gaus.)	Island		1	0.057	0.811
				Site		1	3.698	0.054
				Island:Site		1	0.063	0.802
LC-MUFA /%	Pocillopora	Host	ANOVA	(Intercept)	450.12	1	886.613	**<0.001**
				Island	0.03	1	0.049	0.827
				Site	0.00	1	0	0.989
				Island:Site	0.00	1	0.005	0.944
				Residuals	23.86	47		
		Symbiont	ANOVA	(Intercept)	136.94	1	210.249	**<0.001**
				Island	0.72	1	1.111	0.298
				Site	3.72	1	5.707	**0.021**
				Island:Site	2.13	1	3.268	0.078
				Residuals	28.01	43		
	Porites	Host	ANOVA	(Intercept)	80.05	1	140.561	**<0.001**
				Island	1.01	1	1.765	0.192
				Site	0.05	1	0.091	0.765
				Island:Site	0.01	1	0.013	0.909
				Residuals	21.64	38		
		Symbiont	ANOVA	(Intercept)	57.93	1	63.043	**<0.001**
				Island	0.60	1	0.649	0.426
				Site	0.22	1	0.24	0.627

DV	Species	Faction	Test		Sum Sq	Df	F value/ LR Chisq	p-value
LC-MUFA /%	Porites	Symbiont	ANOVA	Island:Site	0.07	1	0.074	0.788
				Residuals	32.16	35		
PUFA : SFA	Pocillopora	Host	ANOVA	(Intercept)	9.28	1	1258.767	**<0.001**
				Island	0.00	1	0.209	0.65
				Site	0.00	1	0.107	0.745
				Island:Site	0.02	1	3.18	0.081
				Residuals	0.35	47		
		Symbiont	ANOVA	(Intercept)	16.99	1	361.538	**<0.001**
				Island	0.00	1	0.002	0.965
				Site	0.06	1	1.295	0.261
				Island:Site	0.24	1	5.079	**0.029**
				Residuals	2.02	43		
	Porites	Host	ANOVA	(Intercept)	11.82	1	839.458	**<0.001**
				Island	0.17	1	11.774	**0.001**
				Site	0.06	1	4.38	**0.043**
				Island:Site	0.01	1	0.911	0.346
				Residuals	0.54	38		
		Symbiont	ANOVA	(Intercept)	18.46	1	298.705	**<0.001**
				Island	0.59	1	9.58	**0.004**
				Site	0.74	1	11.942	**0.001**
				Island:Site	0.03	1	0.414	0.524
				Residuals	2.10	34		

Supplement Table 7: Results of post hoc estimated marginal means with Tukey HSD correction for trophic markers. Models for separated Pocillopora and Porites host and symbiont fractions. Significant values (p<0.05) in bold. Mi = Miang, Ra = Racha.

DV	Species	Faction	contrast	estimate	SE	df	t-ratio / z-ratio	p-value
Animal derived : PS derived FA	Porites	Host	Mi E - Ra E	7.25	3.89	38	1.86	0.261
			Mi E - Mi W	-5.42	4.07	38	-1.33	0.548
			Mi E - Ra W	2.01	3.71	38	0.54	0.948
			Ra E - Mi W	-12.67	3.76	38	-3.37	**0.009**
			Ra E - Ra W	-5.24	3.37	38	-1.55	0.418
			Mi W - Ra W	7.44	3.58	38	2.08	0.179
C18:1n-9 : C18:1n-7	Porites	Host	Mi E - Ra E	-2.92	7.70	38	-0.38	0.981
			Mi E - Mi W	12.11	8.05	38	1.50	0.445
			Mi E - Ra W	3.18	7.34	38	0.43	0.973
			Ra E - Mi W	15.02	7.45	38	2.02	0.200
			Ra E - Ra W	6.09	6.68	38	0.91	0.798
			Mi W - Ra W	-8.93	7.08	38	-1.26	0.593
		Symbiont	Mi E - Ra E	-191.05	109.41	35	-1.75	0.316
			Mi E - Mi W	0.75	117.12	35	0.01	1.000
			Mi E - Ra W	-10.21	106.09	35	-0.10	1.000
			Ra E - Mi W	191.81	105.15	35	1.82	0.279

DV	Species	Faction	contrast	estimate	SE	df	t-ratio / z-ratio	p-value
C18:1n-9 : C18:1n-7	Porites	Symbiont	Ra E - Ra W	180.84	92.70	35	1.95	0.226
			Mi W - Ra W	-10.97	101.69	35	-0.11	1.000
EPA : DHA	Pocillopora	Host	Mi E - Ra E	-0.02	0.03	47	-0.68	0.906
			Mi E - Mi W	-0.06	0.03	47	-2.02	0.194
			Mi E - Ra W	0.00	0.03	47	0.12	0.999
			Ra E - Mi W	-0.04	0.03	47	-1.52	0.434
			Ra E - Ra W	0.02	0.03	47	0.82	0.843
			Mi W - Ra W	0.06	0.03	47	2.19	0.140
		Symbiont	Mi E - Ra E	-0.02	0.07	43	-0.23	0.996
			Mi E - Mi W	0.13	0.08	43	1.63	0.373
			Mi E - Ra W	-0.23	0.08	43	-2.86	**0.032**
			Ra E - Mi W	0.15	0.07	43	1.98	0.211
			Ra E - Ra W	-0.22	0.08	43	-2.84	**0.034**
			Mi W - Ra W	-0.36	0.08	43	-4.45	**0.000**
	Porites	Host	Mi E - Ra E	0.41	0.59	38	0.70	0.895
			Mi E - Mi W	-0.96	0.81	38	-1.18	0.643
			Mi E - Ra W	-0.89	0.70	38	-1.27	0.589
			Ra E - Mi W	-1.37	0.73	38	-1.87	0.256
			Ra E - Ra W	-1.30	0.61	38	-2.14	0.160
			Mi W - Ra W	0.07	0.83	38	0.08	1.000
		Symbiont	Mi E - Ra E	-2.26	1.00	35	-2.25	0.130
			Mi E - Mi W	-4.76	1.47	35	-3.24	**0.013**
			Mi E - Ra W	-1.70	0.90	35	-1.89	0.252
			Ra E - Mi W	-2.50	1.55	35	-1.61	0.387
			Ra E - Ra W	0.56	1.04	35	0.54	0.949
			Mi W - Ra W	3.05	1.49	35	2.05	0.189
LC MUFA / %	Pocillopora	Symbiont	Mi E - Ra E	-0.18	0.32	43	-0.56	0.943
			Mi E - Mi W	-1.00	0.34	43	-2.91	**0.028**
			Mi E - Ra W	-0.32	0.35	43	-0.90	0.804
			Ra E - Mi W	-0.82	0.32	43	-2.56	0.065
			Ra E - Ra W	-0.14	0.33	43	-0.42	0.975
			Mi W - Ra W	0.68	0.35	43	1.93	0.230
PUFA : SFA	Pocillopora	Host	Mi E - Ra E	0.05	0.03	47	1.62	0.379
			Mi E - Mi W	0.04	0.04	47	0.99	0.757
			Mi E - Ra W	0.00	0.04	47	0.09	1.000
			Ra E - Mi W	-0.02	0.03	47	-0.58	0.938
			Ra E - Ra W	-0.05	0.03	47	-1.56	0.409
			Mi W - Ra W	-0.03	0.04	47	-0.92	0.795
		Symbiont	Mi E - Ra E	0.14	0.09	43	1.64	0.366
			Mi E - Mi W	0.07	0.09	43	0.77	0.866
			Mi E - Ra W	-0.08	0.10	43	-0.80	0.855
			Ra E - Mi W	-0.07	0.09	43	-0.81	0.848

DV	Species	Faction	contrast	estimate	SE	df	t-ratio / z-ratio	p-value
PUFA : SFA	Pocillopora	Symbiont	Ra E - Ra W	-0.22	0.09	43	-2.45	0.082
			Mi W - Ra W	-0.15	0.10	43	-1.55	0.416
	Porites	Host	Mi E - Ra E	0.09	0.06	38	1.68	0.347
			Mi E - Mi W	-0.11	0.06	38	-1.98	0.214
			Mi E - Ra W	0.05	0.05	38	0.95	0.776
			Ra E - Mi W	-0.21	0.05	38	-3.88	**0.002**
			Ra E - Ra W	-0.04	0.05	38	-0.89	0.809
			Mi W - Ra W	0.16	0.05	38	3.24	**0.013**
		Symbiont	Mi E - Ra E	0.20	0.12	34	1.69	0.347
			Mi E - Mi W	-0.34	0.13	34	-2.63	0.058
			Mi E - Ra W	-0.03	0.12	34	-0.25	0.994
			Ra E - Mi W	-0.54	0.12	34	-4.69	**0.000**
			Ra E - Ra W	-0.23	0.10	34	-2.24	0.133
			Mi W - Ra W	0.31	0.11	34	2.72	**0.048**
Total FA / surface	Pocillopora	Symbiont	Mi E - Ra E	-18.87	17.88	43	-1.06	0.718
			Mi E - Mi W	-65.39	19.21	43	-3.41	**0.008**
			Mi E - Ra W	-27.17	19.68	43	-1.38	0.518
			Ra E - Mi W	-46.51	17.88	43	-2.60	0.059
			Ra E - Ra W	-8.30	18.39	43	-0.45	0.969
			Mi W - Ra W	38.22	19.68	43	1.94	0.226
	Porites	Host	Mi E - Ra E	-4.50	56.80	38	-0.08	1.000
			Mi E - Mi W	-134.68	59.40	38	-2.27	0.124
			Mi E - Ra W	-96.47	54.18	38	-1.78	0.298
			Ra E - Mi W	-130.18	54.94	38	-2.37	0.101
			Ra E - Ra W	-91.97	49.25	38	-1.87	0.259
			Mi W - Ra W	38.21	52.23	38	0.73	0.884

Statutory Declaration

Statutory declaration/ Eidesstattliche Erklärung

I declare that I have developed and written the enclosed Master Thesis by myself and have not used sources or means without declaring them. Any thoughts from others or literal quotations are clearly marked. The Master Thesis was not used in the same or in a similar version to achieve an academic grading or is being published elsewhere. The written version is identical to the Version on the DVD/USB Drive.

Hiermit erkläre ich, dass ich die vorliegende Arbeit selbstständig angefertigt und keine anderen als die angegebenen Quellen und Hilfsmittel verwendet habe.

Weiterhin versichere ich, dass diese Arbeit noch nicht als Abschlussarbeit an anderer Stelle vorgelegen wurde. Die eingereichte schriftliche Fassung der Arbeit entspricht der Fassung auf dem elektronischen Speichermedium.

_____

Location, Date, Signature

Ort, Datum, Unterschrift